

# Liposome-Encapsulated Doxorubicin Reverses Drug Resistance by Inhibiting P-Glycoprotein in Human Cancer Cells

Chiara Riganti,<sup>\*,†,‡</sup> Claudia Voena,<sup>‡,§</sup> Joanna Kopecka,<sup>†</sup> Paola Antonia Corsetto,<sup>||</sup> Gigliola Montorfano,<sup>||</sup> Emanuele Enrico,<sup>⊥</sup> Costanzo Costamagna,<sup>†</sup> Angela Maria Rizzo,<sup>||</sup> Dario Ghigo,<sup>†,‡</sup> and Amalia Bosia<sup>†,‡</sup>

<sup>†</sup>Department of Genetics, Biology and Biochemistry, University of Torino, Torino, Italy

<sup>‡</sup>Research Center on Experimental Medicine (Ce.R.M.S.), University of Torino and San Giovanni Battista Hospital, Torino, Italy

<sup>§</sup>Department of Biomedical Sciences and Human Oncology, University of Torino, Torino, Italy

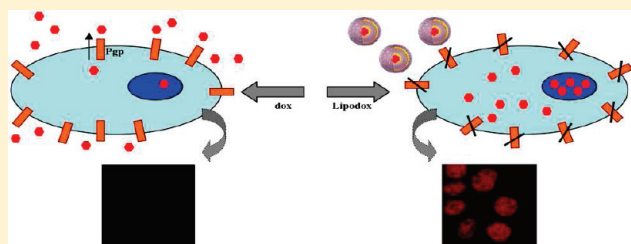
<sup>||</sup>Department of Molecular Science Applied to Biosystems (DISMAB), University of Milano, Milano, Italy

<sup>⊥</sup>National Institute of Metrologic Research, Electromagnetism Division, Quantum Research Laboratories and Nanofacility Piemonte, Torino, Italy

**S** Supporting Information

**ABSTRACT:** The most frequent drawback of doxorubicin is the onset of drug resistance, due to the active efflux through P-glycoprotein (Pgp). Recently formulations of liposome-encapsulated doxorubicin have been approved for the treatment of tumors resistant to conventional anticancer drugs, but the molecular basis of their efficacy is not known. To clarify by which mechanisms the liposome-encapsulated doxorubicin is effective in drug-resistant cancer cells, we analyzed the effects of doxorubicin and doxorubicin-containing anionic liposomal nanoparticles ("Lipodox") on the drug-sensitive human colon cancer HT29 cells and on the drug-resistant HT29-dx cells. Interestingly, we did not detect any difference in drug accumulation and toxicity between free doxorubicin and Lipodox in HT29 cells, but Lipodox was significantly more effective than doxorubicin in HT29-dx cells, which are rich in Pgp. This effect was lost in HT29-dx cells silenced for Pgp and acquired by HT29 cells overexpressing Pgp. Lipodox was less extruded by Pgp than doxorubicin and inhibited the pump activity. This inhibition was due to a double effect: the liposome shell per se altered the composition of rafts in resistant cells and decreased the lipid raft-associated amount of Pgp, and the doxorubicin-loaded liposomes directly impaired transport and ATPase activity of Pgp. The efficacy of Lipodox was not increased by verapamil and cyclosporin A and was underwent interference by colchicine. Binding assays revealed that Lipodox competed with verapamil for binding Pgp and hampered the interaction of colchicine with this transporter. Site-directed mutagenesis experiments demonstrated that glycine 185 is a critical residue for the direct inhibitory effect of Lipodox on Pgp. Our work describes novel properties of liposomal doxorubicin, investigating the molecular bases that make this formulation an inhibitor of Pgp activity and a vehicle particularly indicated against drug-resistant tumors.

**KEYWORDS:** doxorubicin, liposomes, P-glycoprotein, multidrug resistance



## INTRODUCTION

Doxorubicin is an anthracycline widely used to treat solid and hematological tumors, but its major drawback is the onset of resistance. Being a substrate for several ATP-binding cassette (ABC) membrane transporters, such as P-glycoprotein (Pgp), multidrug-resistance related protein-1 and -2, and breast cancer resistance protein, the drug is actively extruded from cells overexpressing these pumps and has a low intracellular retention.<sup>1,2</sup> To circumvent drug resistance, several inhibitors of Pgp have been designed, including verapamil, cyclosporin A and PSC 833.<sup>1</sup> The poor specificity and the high toxicity of these compounds have determined negative results in clinical trials.<sup>3</sup> Therefore, the research of effective and nontoxic chemoresistance-reversing strategies is a field of extensive investigations.<sup>4–6</sup>

Pgp has multiple binding sites for substrates and modulators. Each site can oscillate from a low-affinity state to a high-affinity state, and the presence of the ligand on one site can allosterically modulate the other sites.<sup>7</sup> It is not rare that compounds theoretically acting as modulators bind to the sites for classical substrates,<sup>7</sup> making difficult our knowledge about drug transport and inhibition mechanisms of Pgp.

Recently doxorubicin-loaded liposomes have been demonstrated to be effective against aggressive tumors, like breast and ovary metastatic cancers<sup>8</sup> and recurrent glioblastoma.<sup>9</sup>

**Received:** July 29, 2010

**Accepted:** April 14, 2011

**Published:** April 14, 2011

Liposomes have several advantages in comparison with non-encapsulated chemotherapeutic drugs: for instance, the liposomal nanoparticles show a preferential accumulation within the cancer sites, are less cleared than free drugs, can be conjugated with specific ligands of tumor-associated receptors, can be loaded with multiple anticancer drugs and chemosensitizers, and can be designed to exert the maximal activity at the intracellular pH of tumors.<sup>10,11</sup> Liposome-encapsulated drugs also display a good efficacy against drug-resistant tumors. A liposomal formulation of doxorubicin is cytotoxic in resistant small cell lung cancer SBC-3 cells<sup>12</sup> and reduces the tumor growth of the resistant ovarian A2780/AD cells<sup>13</sup> and of colon CT26/DOX cells<sup>14</sup> implanted in mice. In parallel, doxorubicin-loaded liposomes have shown a better therapeutic index than free doxorubicin in patients with metastatic breast cancers, characterized by a poor response to chemotherapy,<sup>15</sup> and in patients with non-Hodgkin's lymphoma, a tumor that is often chemoresistant.<sup>16</sup>

Liposomes have been proposed to grant an easier delivery of the anticancer drugs into the nucleus<sup>17</sup> and a release for longer time periods.<sup>12</sup> In addition, when loaded into liposomes, doxorubicin is less potent than free doxorubicin in upregulating Pgp expression in cancer cells<sup>13</sup> and can also target the tumor microenvironment, inducing the preferential apoptosis of vascular endothelium of drug-resistant tumors.<sup>14</sup> Liposomes inhibit the binding of vincristine to Pgp, suggesting a direct interaction between the liposome shell and the pump.<sup>18,19</sup> However, the functional consequences of this putative interaction on Pgp activity have not been yet fully clarified.

In this work we demonstrated that the accumulation and the cytotoxicity of doxorubicin-loaded liposomes ("Lipodox") correlates with the expression of Pgp, showing that Lipodox interacts with one of the drug-binding sites of Pgp, inhibits the efflux activity, and alters the membrane microenvironment where Pgp works.

## MATERIALS AND METHODS

**Chemicals.** Fetal bovine serum (FBS) and culture medium were supplied by Invitrogen Life Technologies (Carlsbad, CA); plasticware for cell cultures was from Falcon (Becton Dickinson, Franklin Lakes, NJ). Rhodamine 123 and Hoechst 33342 were purchased from Calbiochem (San Diego, CA). Electrophoresis reagents were obtained from Bio-Rad Laboratories (Hercules, CA); the protein content of cell monolayers and lysates was assessed with the BCA kit from Sigma Chemical Co. (St. Louis, MO). [<sup>3</sup>H]verapamil and [<sup>3</sup>H]colchicine were from PerkinElmer (Waltham, MA). When not otherwise specified, all the other reagents were purchased from Sigma Chemical Co.

**Cell Lines.** Human colon cancer HT29 cells were cultured in RPMI 1640 medium. A subpopulation of HT29 cells, named HT29-dx, was created as previously reported<sup>20</sup> and subsequently cultured in RPMI 1640 medium containing 150 nmol/L doxorubicin. HT29-dx cells exhibited a higher amount of Pgp, had a lower intracellular accumulation of doxorubicin and were more resistant to the drug toxic effects, if compared to HT29 cells.<sup>20</sup> Human doxorubicin-sensitive lung cancer A549 cells and doxorubicin-resistant A549-dx cells (selected from the parental A549 cells after 30 passages in the presence of 50 nmol/L doxorubicin) were grown in HAM'S F12 medium. Human doxorubicin-sensitive breast cancer MCF-7 cells and doxorubicin resistant MCF-7-dx cells (obtained by transfecting the parental MCF-7 with pCDNA3 expression vector, provided by Invitrogen Life

Technologies, containing the whole cDNA of *mdr1* gene, which encodes for human Pgp) were cultured in RPMI 1640 medium. MM98 cells, a primary malignant mesothelioma cell culture established from the pleural effusion of a patient with histologically confirmed malignant mesothelioma, were already described.<sup>21</sup> All the culture mediums were supplemented with 10% FBS, 1% penicillin–streptomycin (PS) and 1% L-glutamine. Cell cultures were maintained in a humidified atmosphere at 37 °C and 5% CO<sub>2</sub>.

**Liposome Synthesis and Characterization.** Anionic liposomes (COATSOME EL-01-PA, from NOF Corporation, Tokyo, Japan, with the following composition: 1,2-distearoyl-*sn*-glycero-3-phosphoethanolamine conjugated with polyethylene glycol, cholesterol, 1,2-dipalmitoyl-*sn*-glycero-3-phosphocoline, 1,2-dipalmitoyl-*sn*-glycero-3-phosphoglycerol, with a ratio 4.2: 11.4: 15.2: 11.4, 29 mg total lipids) were incubated with 1.5 mmol/L doxorubicin in sterile aqueous solution, according to the manufacturer's instructions. The residual non-encapsulated drug was removed by gel filtration using a Sephadex G-50 (Amersham Bioscience, Piscataway, NJ) column. The amount of encapsulated doxorubicin was quantified by measuring the fluorescence emitted as reported below; the encapsulation efficiency was calculated as described.<sup>22</sup> The liposomes with an encapsulation efficiency higher than 85%, termed Lipodox, were collected and used for all the experimental procedures.

The liposome dimensions were evaluated by dynamic light scattering. Ten microliters of the liposome suspension was diluted in 1 mL of 120 mmol/L NaCl solution and analyzed with an ALV-NIBS dynamic light scattering instrument (Langen, Germany) provided with a Ne–He laser and an ALV-5000 multiple tau digital correlator. The scattered light intensity was recorded for 30 s on suspensions at 25 °C. The hydrodynamic radius of liposomes was evaluated by using both the cumulant method and the CONTIN algorithm.<sup>23</sup>

To visualize the nanoparticle morphology, liposomes were diluted at 5 mg/mL concentration in 0.9% w/v NaCl solution and analyzed with a Philips CM10 transmission electron microscope (TEM) operating at an acceleration voltage of 80 kV. Scanning electron microscopy (SEM) images were obtained with a Quanta 3D FEG DualBeam microscope (Fei Company, Hillsboro, OR); nanometric resolution was obtained with the Field Emission electron source operating at an acceleration voltage of 5 kV. For each sample a minimum of 3 microscopic fields were examined.

**Intracellular Doxorubicin Accumulation and Efflux.** Cells were grown in 35 mm diameter Petri dishes and incubated in fresh medium containing doxorubicin or Lipodox, as reported in Results. The intracellular accumulation of doxorubicin was detected using a PerkinElmer LS-5 spectrofluorimeter, as described.<sup>20</sup> To measure the doxorubicin efflux, cells were incubated for 20 min with doxorubicin or Lipodox, then washed five times with PBS and rinsed with 1 mL of fresh PBS. Aliquots of extracellular supernatant were collected at time zero (*t*<sub>0</sub>) and at fixed time points (up to 30 min), and checked for the doxorubicin amount. Fluorescence was converted in nmol of doxorubicin/mg of cell proteins using a calibration curve prepared previously.

Kinetic parameters were calculated as reported earlier.<sup>20</sup> HT29 Pgp<sup>+</sup> cells were incubated for 20 min with increasing amounts of doxorubicin, Lipodox or [<sup>3</sup>H]colchicine, then washed and analyzed for the intracellular concentration of the drugs. In parallel a second series of dishes, after the incubation with doxorubicin, Lipodox and [<sup>3</sup>H]colchicine under the same experimental conditions, were left for a further 10 min at 37 °C, then washed and

tested for the intracellular drug content. The difference of drug concentration between the two series, expressed as nmol extruded/min/mg of protein for doxorubicin and Lipodox and as  $\mu\text{mol}$  extruded/min/mg of protein for [ $^3\text{H}$ ]colchicine, was plotted versus the initial drug concentration. Values were fitted to the Michaelis–Menten equation to calculate  $V_{\text{max}}$  and  $K_m$ , using the Enzfitter software (Biosoft Corporation, Cambridge, United Kingdom).

**Immunofluorescence Staining.**  $0.5 \times 10^6$  cells, incubated in the experimental conditions reported in Results, were grown on sterile glass coverslips, rinsed with PBS, fixed with 4% w/v paraformaldehyde (diluted in PBS), washed three times with PBS and incubated with 4',6-diamidino-2-phenylindole dihydrochloride (DAPI, diluted 1:20000). Fluorescently labeled cells were washed three times with PBS and once with water, and then the slides were mounted with 4  $\mu\text{L}$  of Gel Mount Aqueous Mounting and examined with a Leica DC100 fluorescence microscope (Leica Microsystems GmbH, Wetzlar, Germany). For each experimental point, a minimum of 5 microscopic fields were examined.

**Cytotoxicity Assays.** After incubation under different experimental conditions (see Results), the lactate dehydrogenase (LDH) activity was measured in the extracellular medium and in the cell lysate, as previously described,<sup>20</sup> to check the cytotoxicity of the drugs. Under the same experimental conditions, cells were checked for annexin V–fluorescein isothiocyanate (FITC) positivity, chosen as an index of apoptosis,<sup>21</sup> using a FACSCalibur system (Becton Dickinson), with a 530 nm band-pass filter. For each analysis 100,000 events were collected and the percentage of cells positive for annexin V–FITC was calculated by the CellQuest software (Becton Dickinson). For  $\text{IC}_{50}$  determination, cells were incubated with increasing concentrations of doxorubicin or Lipodox and the extracellular LDH activity was detected. Using the Trypan-blue exclusion method we previously assessed that percentage of HT29 dead cells incubated for 24 h with 50  $\mu\text{mol/L}$  doxorubicin was 0% cytotoxicity (data not shown). The LDH activity corresponding to this experimental condition was taken as 100%, and the LDH values of all the other experimental points were expressed accordingly.  $\text{IC}_{50}$  was defined as the amount of doxorubicin or Lipodox which gave 50% of the maximal LDH release after 24 h.

**Cell Transfection and Silencing.** The pHa vector containing the complete *mdr1* cDNA was purchased from Addgene (Cambridge, MA) and subcloned into pCDNA3 vector as described.<sup>24</sup> By sequencing the *mdr1* gene present in the pCDNA3 vector, we verified that it contained the codon GGA (nucleotides 553–555), codifying for glycine at position 185 of the protein (data not shown). In transfection experiments  $2 \times 10^5$  HT29 cells were treated with 6  $\mu\text{L}$  of jetPEI transfection reagent (Polyplus-transfection SA BIOPARC, Illkirch, France) and 3  $\mu\text{g}$  of DNA *mdr1*-pCDNA3 or empty-pCDNA3.

To silence Pgp in HT29-dx cells,  $2 \times 10^5$  cells were incubated with 50 pmol of Pgp siRNA (Santa Cruz Biotechnology Inc., Santa Cruz, CA) and 5  $\mu\text{L}$  of siRNA transfection reagent (Santa Cruz Biotechnology Inc.). In each set of experiments, one dish was treated with 50 pmol of Control siRNA-A (Santa Cruz Biotechnology Inc.), a scrambled nontargeting 20- to 25-nucleotide siRNA designed as a negative control. To assess the efficacy of transfection and silencing, the expression of Pgp was analyzed by Western blotting, as reported below. Cell viability was not affected by the procedures, because the LDH release in the supernatant after 24, 48, and 72 h from the transfected or silenced cells was the same as in nontransfected cells (data not shown).

**Western Blot.** Cells were rinsed with 0.5 mL of boiling lysis buffer (10 mmol/L Tris, 100 mmol/L NaCl, 20 mmol/L  $\text{KH}_2\text{PO}_4$ , 30 mmol/L EDTA, 1 mmol/L EGTA, 250 mmol/L sucrose; pH 7.5). After sonication 1 mmol/L  $\text{Na}_3\text{VO}_4$ , 1 mmol/L NaF, 1 mmol/L 4-(2-aminoethyl)benzenesulfonyl fluoride, 10 mmol/L dithiothreitol and the inhibitor cocktail set III (100 mmol/L AEBSF, 80 mmol/L aprotinin, 5 mmol/L bestatin, 1.5 mmol/L E-64, 2 mmol/L leupeptin and 1 mmol/L pepstatin; Calbiochem) were added and cell lysates were centrifuged at 13000g for 15 min. Cell proteins (30  $\mu\text{g}$ ) were separated by SDS–PAGE and probed with an anti-Pgp antibody (from rabbit, diluted 1:250 in PBS–milk 3%, Santa Cruz Biotechnology) and with an anti-glyceraldehyde 3-phosphate dehydrogenase (GAPDH) antibody (from rabbit, diluted 1:500 in PBS–BSA 1%, Santa Cruz Biotechnology), used as control of equal loading. For lipid raft samples, we used 5  $\mu\text{g}$  of proteins in Western blot experiments for Pgp. Proteins were detected by enhanced chemiluminescence (Immun-Star, Bio-Rad).

**Pgp Activity.** The efflux of rhodamine 123, a specific substrate of Pgp,<sup>2</sup> was taken as an index of Pgp activity. Cells were grown for 3 h in fresh medium, or in the presence of doxorubicin, empty liposomes or Lipodox. This experimental condition allowed Lipodox to accumulate within drug-resistant cells at an amount superimposable to drug-sensitive cells (see Results). Cells were then washed with fresh PBS, detached with cell dissociation solution and resuspended at  $5 \times 10^5$  cells/mL in 1 mL of RPMI medium containing 5% FBS. The samples were maintained at 37 °C for 20 min in the presence of 1  $\mu\text{g/mL}$  rhodamine 123. After this incubation time, cells were washed and resuspended in 0.5 mL of PBS, and the intracellular rhodamine content, which is inversely related to its efflux, was detected using a FACSCalibur system (Becton Dickinson). For each analysis 100,000 events were collected and data were analyzed by the CellQuest software (Becton Dickinson).

A second assay of Pgp activity was the detection of the intracellular accumulation of Hoechst 33342. Cells were washed with PBS and resuspended in 0.5 mL of DPBS buffer (129 mmol/L NaCl, 2.5 mmol/L KCl, 7.4 mmol/L  $\text{Na}_2\text{HPO}_4$ , 1.3 mmol/L  $\text{KH}_2\text{PO}_4$ , 1 mmol/L  $\text{CaCl}_2$ , 0.7 mmol/L  $\text{MgSO}_4$ , 5.3 mmol/L glucose; pH 7.4), in the presence of 50  $\mu\text{mol/L}$  Hoechst 33342 for 15 min at 37 °C. Then 0.4 mL of stop solution (210 mmol/L KCl, 2 mmol/L Hepes; pH 7.4) was added and cells were lysed with 0.1 mL of 0.1% v/v Triton-X 100, dissolved in 0.3% v/v NaOH. An aliquot of sample was used for the determination of the intracellular proteins, and the remaining part was analyzed for the Hoechst content, using a PerkinElmer LS-5 spectrofluorimeter. Excitation and emission wavelengths were 370 and 450 nm, respectively. A blank was prepared in the absence of cells in each set of experiments, and its fluorescence was subtracted from the one measured in each sample. Fluorescence was converted in nmol of Hoechst/mg of cell proteins using a calibration curve prepared previously.

**ATPase Assay.** The assay was performed on Pgp-rich membrane vesicles according to Litman et al.<sup>25</sup> with minor modifications. Cells were washed with Ringer's solution (148.7 mmol/L NaCl, 2.55 mmol/L  $\text{K}_2\text{HPO}_4$ , 0.45 mmol/L  $\text{KH}_2\text{PO}_4$ , 1.2 mmol/L  $\text{MgSO}_4$ , pH 7.4), lysed on crushed ice with lysis buffer (10 mmol/L Hepes/Tris, 5 mmol/L EDTA, 5 mmol/L EGTA, 2 mmol/L dithiothreitol, pH 7.4) supplemented with 2 mmol/L phenylmethylsulfonyl fluoride, 1 mmol/L aprotinin, 10  $\mu\text{g/mL}$  pepstatin, 10  $\mu\text{g/mL}$  leupeptin, and subjected to nitrogen cavitation at 1200 psi for 20 min. Samples were



centrifuged at 300g for 10 min, diluted 1:4 in the precentrifugation buffer (10 mmol/L Tris/HCl, 25 mmol/L sucrose, pH 7.5), overlaid on a 35% sucrose cushion (10 mmol/L Tris/HCl, 35% w/v sucrose, 1 mmol/L EDTA, pH 7.5) and centrifuged at 14000g for 10 min. The interface was collected, diluted 1:5 in the centrifugation buffer (10 mmol/L Tris/HCl, 250 mmol/L sucrose, pH 7.5) and subjected to a third centrifugation at 100000g for 45 min. The vesicle pellet was resuspended in 0.5 mL of centrifugation buffer and stored at  $-80^{\circ}\text{C}$  until use, after the quantification of the protein content. For ATPase assays, samples (containing 20  $\mu\text{g}$  of protein) were incubated for 30 min at  $37^{\circ}\text{C}$  with 50  $\mu\text{L}$  of the reaction mix (25 mmol/L Tris/HCl, 3 mmol/L ATP, 50 mmol/L KCl, 2.5 mmol/L  $\text{MgSO}_4$ , 3 mmol/L dithiothreitol, 0.5 mmol/L EGTA, 2 mmol/L ouabain, 3 mmol/L sodium azide, pH 7.0), in the absence or presence of doxorubicin, empty liposomes, Lipodex, cyclosporin A,  $\text{Na}_3\text{VO}_4$ , verapamil or colchicine, in the combinations indicated in Results. In each set of experiments, a blank containing 0.5 mmol/L  $\text{Na}_3\text{VO}_4$  was included. The reaction was stopped by adding 0.2 mL of ice-cold stopping buffer (0.2% w/v ammonium molybdate, 1.3% v/v  $\text{H}_2\text{SO}_4$ , 0.9% w/v SDS, 2.3% w/v trichloroacetic acid, 1% w/v ascorbic acid). After a 30 min incubation at room temperature, the absorbance of the phosphate hydrolyzed from ATP was measured at 620 nm, using a Packard EL340 microplate reader (Bio-Tek Instruments, Winooski, MA). The absorbance was converted into  $\mu\text{mol}$  of hydrolyzed  $\text{P}_i$ /min/mg of protein, according to the titration curve previously prepared. Values were fitted to Michaelis–Menten equation to calculate  $K_m$ , using the Enzfitter software.

**Lipid Raft Isolation and Analysis.** Cells were harvested in PBS containing 0.4 mmol/L  $\text{Na}_3\text{VO}_4$  and resuspended in 1.4 mL of lysis buffer (1% v/v Triton X-100, 10 mmol/L Tris/HCl, 150 mmol/L NaCl, 5 mmol/L EDTA, 1 mmol/L  $\text{Na}_3\text{VO}_4$ , 1 mM phenylmethylsulfonyl fluoride, 75 mU/mL aprotinin, pH 7.5). After a 20 min incubation on ice, they were homogenized with a Dounce homogenizer (10 strokes, tight). Cell lysate was centrifuged at 1300g for 5 min, and 1 mL of supernatant was mixed with an equal volume of 85% w/v sucrose in 10 mmol/L Tris/HCl, 150 mmol/L NaCl, 5 mmol/L EDTA, 1 mmol/L  $\text{Na}_3\text{VO}_4$ , pH 7.5, and then overlaid on 5.5 mL of 30% w/v sucrose and 4 mL of 5% w/v sucrose. Samples were centrifuged at 200000g for 17 h at  $4^{\circ}\text{C}$  in Optimal LE-80K Ultracentrifuge (TST-41.14 rotor, Beckman Coulter, Brea, CA). Eleven fractions were collected: lipid rafts were enriched in fractions 5 and 6, as reported in the literature and confirmed by the presence of flotillin-1, detected by Western blot with a rabbit polyclonal antibody (Santa Cruz Biotechnology Inc.), diluted 1:200 in 5% milk–TBS–Tween).

For lipid analysis, whole and fractionated cells were extracted with three different chloroform/methanol mixtures, 1:1, 1:2, 2:1 (v/v), partitioned with the upper phase (chloroform/methanol/water, 47:48:1, v/v/v) and then with water. After partitioning, the organic phase was dried and resuspended in chloroform/methanol (2:1 v/v) for the analysis of phospholipids. Purification of phospholipid moieties was obtained using a HPLC evaporative light scattering detector system (Jasco, Japan) equipped with one pump, a SCL-10 Advp, a degasser module, a Rheodyne manual injector with 20  $\mu\text{L}$  sample loop, a column (250 mm  $\times$  4.6 mm  $\times$  I.D., 5  $\mu\text{m}$ ) packed with silica normal-phase LiChrospher Si 60 (LiChroCART 250–4, Merck, Darmstadt, Germany). The chromatographic separation was carried out using a linear binary gradient according to the following scheme:  $t_0$  min, 0% B;

$t_{14}$  min, 100% B; and finally isocratic conditions (100% B) for 9 min. Total chromatographic run time was 40 min per sample, which consists of 23 min analysis, 12 min to restore initial conditions and 5 min for re-equilibration. Eluent A was chloroform–methanol–water (80:19.5:0.5, v/v/v), and eluent B was chloroform–methanol–water (60:34.6:1 v/v/v). The flow rate of the eluent was 1.0 mL/min. After elution, each sample was split in two aliquots, with a 1:9 ratio, i.e. one part to the detector and nine parts to the Gilson Fraction Collector model 201, in order to collect the different phospholipid classes for further gas chromatography analysis. Phospholipid-derived fatty acids were determined as methyl esters by gas chromatography. The methyl esters were obtained by reaction with sodium methoxide in 3.33% w/v methanol and injected into a gas chromatograph (Agilent Technologies 6850 series II, Agilent, Santa Clara, CA), equipped with a flame ionization detector, under the following conditions: capillary column AT Silar length 30 m, film thickness 0.25  $\mu\text{m}$ , gas carrier helium, temperatures of injector  $250^{\circ}\text{C}$ , detector  $275^{\circ}\text{C}$ , oven  $50^{\circ}\text{C}$ , with a rate of  $10^{\circ}\text{C}/\text{min}$  until  $200^{\circ}\text{C}$  for 20 min.

**Verapamil and Colchicine Binding.** Pgp-rich membrane vesicles containing 10  $\mu\text{g}$  of proteins were incubated in Multi-Screen 96-wells plate 0.22  $\mu\text{m}$  pore size (Millipore, Billerica, MA) for 30 min at room temperature with 1.2 nmol/L [ $^3\text{H}$ ]verapamil or 1 nmol/L [ $^3\text{H}$ ]colchicine, in 0.1 mL of binding buffer (50 mmol/L Tris/HCl, pH 7.4), in the absence or presence of different concentrations of doxorubicin, Lipodex or cold ligands, as indicated in Results. The reaction was stopped by adding 0.25 mL of ice-cold wash buffer (20 mmol/L Tris/HCl, 50 mmol/L  $\text{MgSO}_4$ , pH 7.4). Samples were rapidly filtered, and the amount of radioactivity entrapped on filters was detected by liquid scintillation count. The nonspecific binding was quantified by incubating samples with 1 mmol/L rhodamine 123 and was subtracted from the total binding. The radioactivity was converted into fmol of radioligand bound/mg of protein, according to the respective titration curves, and for each experimental point the results were expressed as fraction of the maximal binding capacity ( $B_{\text{max}}$ ).

**Site-Directed Mutagenesis.** pCDNA3 vector containing the wild-type *mdr1* cDNA, was subjected to PCR-based mutagenesis using the QuikChange kit (Stratagene, La Jolla, CA), following the manufacturer's instructions. The nucleotides at positions 554 and 555 were mutated from GA to TT, yielding the codon GTT (encoding for valine at position 185 in Pgp protein). The mutation was confirmed by DNA sequencing (data not shown).

**Statistical Analysis.** All data in text and figures are provided as means  $\pm$  SD. The results were analyzed by a one-way analysis of variance (ANOVA) and Tukey's test.  $p < 0.05$  was considered significant.

## RESULTS

**Lipodex Accumulates More than Free Doxorubicin in Drug-Resistant HT29-dx Cells.** Anionic empty liposomes were loaded with doxorubicin, in order to obtain Lipodex. The fluorescence of free doxorubicin and Lipodex was assessed, and each solution was stocked at a concentration of 0.5 mmol/L doxorubicin for the subsequent experiments. The dynamic light scattering ( $n = 3$  per each sample group) showed no significant differences in size and polydispersity index between empty liposomes (radius:  $70.01 \pm 26.13$  nm; polydispersity index: 0.164) and Lipodex (radius:  $73.73 \pm 27.54$  nm;

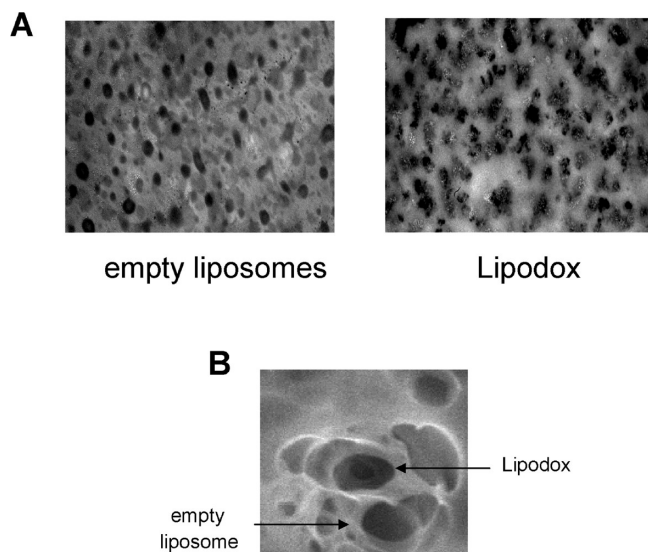


**Figure 1.** Liposomes imaging. (A) TEM microphotographs of empty liposomes and doxorubicin-loaded liposomes (Lipodox). The microphotographs (28500 $\times$  magnification) are representative of three experiments with similar results. (B) SEM microphotographs of liposomes, taken at 100000 $\times$  magnification. The image is representative of three experiments with similar results.

polydispersity index: 0.160), as a consequence of the low molecular weight of doxorubicin compared with the liposomal bulk. In TEM imaging empty liposomes appeared as a round-shaped population, with a homogeneous density; in Lipodox samples, several electron-dense areas, due to the doxorubicin loading, were present within the liposomal envelope (Figure 1A). Analyzing the ultrastructural architecture of liposomes, doxorubicin appeared as a compact concretion, occupying about half the volume of the liposomal shell (Figure 1B).

In dose-dependence experiments we compared the intracellular accumulation of doxorubicin and Lipodox in the drug-sensitive HT29 cells and in the drug-resistant HT29-dx cells: in sensitive cells both drug formulations were accumulated in a similar way as a function of the concentration (Figure 2A). In HT29-dx cells and in the range 0.1–0.5  $\mu\text{mol/L}$  doxorubicin and Lipodox accumulated in a similar way, albeit lower than in HT29 cells. At 1–25  $\mu\text{mol/L}$ , a range of concentrations which exerts cytotoxic effects in drug-sensitive cells,<sup>20</sup> the intracellular amount of doxorubicin remained low, whereas the content of Lipodox was higher and similar to the amount measured in sensitive cells (Figure 2B). The intracellular accumulations of 5  $\mu\text{mol/L}$  doxorubicin and Lipodox were superimposable and increased with time in HT29 cells (Figure 2C), whereas in HT29-dx cells Lipodox accumulated significantly more than doxorubicin at each time point (Figure 2D). The presence of empty liposomes did not affect the intracellular accumulation of doxorubicin: indeed when we coincubated free doxorubicin and empty liposomes, i.e. not containing anthracycline, the drug content was superimposable to the one observed with doxorubicin alone (Figure 2A–D). Fluorescence microscopy images confirmed a clear difference in the accumulation of doxorubicin between HT29 and HT29-dx cells, whereas Lipodox was retained in both drug-sensitive and drug-resistant cells (Figure 2E).

The cytotoxic effect of doxorubicin and Lipodox, evaluated as release of LDH in the extracellular medium, taken as an index of

cytolysis (Figure 3A), and percentage of annexin V-positive cells, taken as an index of apoptosis (Figure 3B), was similar in HT29 cells. In resistant cells doxorubicin did not evoke any significant release of LDH and increased the positivity to annexin V at a lower extent than in sensitive cells. On the contrary, Lipodox in HT29-dx cells increased the release of LDH and the amount of annexin V-positive cells (Figure 3A,B).

**The Accumulation of Lipodox Is Correlated with the Expression of Pgp.** To investigate whether the efficacy of Lipodox was observed only in drug-resistant colon cancer cells or was common to other tumor types, we examined different doxorubicin-sensitive and doxorubicin-resistant cells: as shown in Figure S1 in the Supporting Information, no differences between free doxorubicin and Lipodox were detected in lung cancer A549 cells and in breast cancer MCF-7 cells (Figure S1A in the Supporting Information), which had hardly detectable levels of Pgp (Figure S1B in the Supporting Information). On the contrary, in the resistant counterparts A549-dx and MCF-7-dx cells, as well as in the malignant mesothelioma MM98 cells, all expressing high amounts of Pgp (Figure S1B in the Supporting Information), the retention of doxorubicin was low if we used the free drug and was significantly increased if we employed Lipodox (Figure S1A in the Supporting Information). Taken together, these results suggested that the greater benefit of Lipodox toward free doxorubicin occurs in tumor cells expressing Pgp. To better clarify how the different expression levels of this transporter could mediate the different efficacy of Lipodox, we transfected HT29 cells with an expression vector for Pgp and silenced Pgp in HT29-dx cells by a specific siRNA. The efficacy and the specificity of transfection and silencing procedures are shown in Figure 4A.

The accumulation of free doxorubicin was lower in Pgp-overexpressing ( $Pgp^+$ ) HT29 cells than in wild-type HT29 cells and was higher in Pgp-silenced ( $Pgp^-$ ) HT29-dx cells than in HT29-dx cells (Figure 4B). The intracellular amount of Lipodox did not differ from that of doxorubicin in the cell populations with low amounts of Pgp (wild-type HT29 cells and HT29-dx  $Pgp^-$  cells), but was significantly higher than that of doxorubicin in the cell lines overexpressing Pgp (HT29  $Pgp^+$  cells and wild-type HT29-dx cells). Also the cytotoxicity of Lipodox was higher than that of doxorubicin in the drug-resistant cell populations (Pgp-transfected HT29 cells and wild-type HT29-dx cells) and remained similar to that of doxorubicin in the drug-sensitive cell lines (HT29 cells and Pgp-silenced HT29-dx cells). On the contrary, free doxorubicin was more cytotoxic in HT29 and in HT29-dx  $Pgp^-$  cells than in HT29-dx and in HT29  $Pgp^+$  cells (Figure 4C).

**Lipodox Inhibits the Efflux Activity of Pgp.** Since the presence of Pgp seems to be critical for the differential accumulation of doxorubicin and Lipodox, we wondered whether the two drug formulations were transported by Pgp with a different affinity or affected the activity of Pgp in a different way. To clarify this issue we first measured the efflux of rhodamine 123, a specific substrate of Pgp, in cells pretreated with doxorubicin or Lipodox, analyzing the intracellular retention of rhodamine, which is inversely proportional to its transport rate by Pgp. The efflux of rhodamine was lower in HT29 cells and in HT29-dx  $Pgp^-$  cells, and higher in HT29-dx cells and in HT29  $Pgp^+$  cells; it did not differ between HT29 cells and HT29-dx  $Pgp^-$ , and between HT29-dx cells and HT29  $Pgp^+$  cells (Figure 5A). The addition of doxorubicin did not modify the transport of rhodamine in comparison to untreated cells. No difference in the efflux of rhodamine was observed when Lipodox replaced doxorubicin

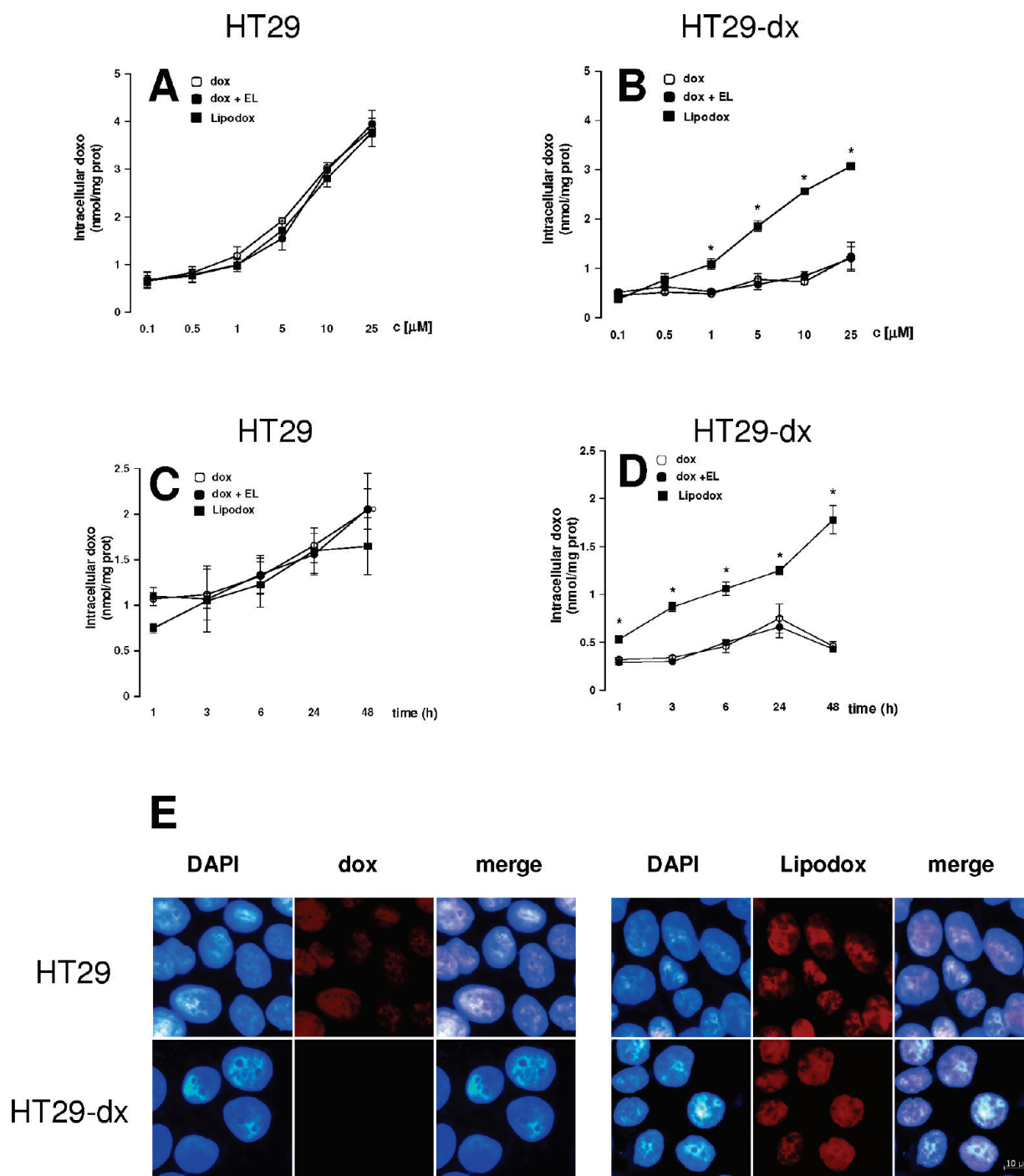


**Figure 2.** Intracellular accumulation of doxorubicin and Lipodox in drug-sensitive and drug-resistant colon cancer cells. HT29 and HT29-dx cells were incubated with doxorubicin (dox, ○), free doxorubicin plus empty liposomes (dox + EL at equimolar concentrations, ●), or doxorubicin-loaded liposomes (Lipodox, ■). (A, B) Different micromolar concentrations of doxorubicin and Lipodox were incubated for 24 h. (C, D) A fixed amount (5 μmol/L) of doxorubicin and Lipodox was incubated for different time periods. The intracellular drug content was assessed fluorimetrically (see Materials and Methods for details). The measurements were performed in triplicate and data are presented as mean ± SD ( $n = 3$ ). Lipodox vs corresponding dox: \* $p < 0.05$ . (E) Nonpermeabilized cells were incubated with 5 μmol/L doxorubicin or Lipodox for 24 h, counterstained with DAPI and analyzed by fluorescence microscopy to detect the intracellular accumulation of doxorubicin. The microphotographs are representative of three experiments with similar results.

in HT29 cells and in HT29-dx  $Pgp^-$  cells, whereas in HT29  $Pgp^+$  cells and HT29-dx cells Lipodox reduced the efflux of the dye (Figure 5A). A superimposable trend was obtained when we measured the intracellular retention of another substrate of  $Pgp$ , Hoechst 33342 dye (Figure 5B), chosen as second assay of  $Pgp$  activity.

We then evaluated the efflux of doxorubicin and Lipodox, after incubating HT29 cells, HT29  $Pgp^+$  cells, HT29-dx cells and HT29-dx  $Pgp^-$  cells for 20 min with 5 μmol/L of both drugs: after this time, the intracellular content of Lipodox did not differ from that of free doxorubicin in each cell population (data not



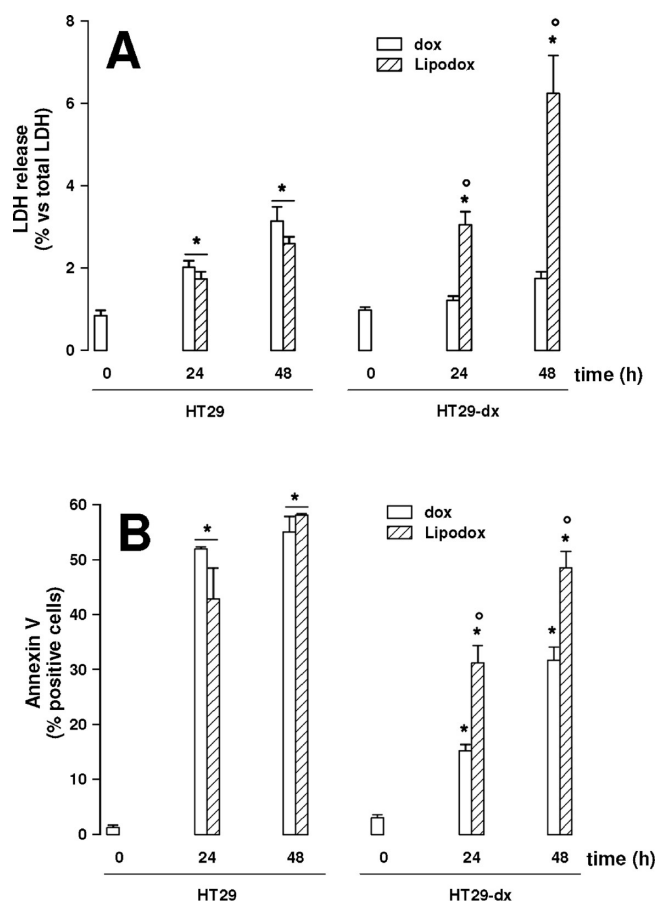


**Figure 3.** Cytotoxicity of Lipodox in drug-sensitive and drug-resistant colon cancer cells. HT29 and HT29-dx cells were grown in the absence (0) or in the presence of 5  $\mu\text{mol/L}$  doxorubicin (dox, open bars) or liposomal doxorubicin (Lipodox, hatched bars) for 24 or 48 h, and then the supernatant was collected and analyzed for the activity of LDH (panel A). Cells were stained with annexin V–FITC and subjected to flow cytometry analysis (panel B), as described in Materials and Methods. The measurements were performed in duplicate, and data are presented as mean  $\pm$  SD ( $n = 3$ ). Vs HT29 or HT29-dx in the absence of drug:  $^*p < 0.01$ . Lipodox vs corresponding dox:  $^{\circ}p < 0.02$ .

shown). As reported in Figure 5C, a saturable efflux of doxorubicin was detected in all the cell groups, reaching a higher velocity in Pgp overexpressing cells (HT29 Pgp<sup>+</sup> and HT29-dx cells). On the contrary, Lipodox extrusion was significantly lower than doxorubicin and hardly detectable in all the cell populations (Figure 5C), suggesting a very low rate of transport by Pgp. Kinetic studies on HT29 Pgp<sup>+</sup> cells exposed to increasing concentrations of doxorubicin or Lipodox revealed that doxorubicin had a  $K_m$  of  $1.85 \pm 0.10 \mu\text{mol/L}$  and a  $V_{\text{max}}$  of  $10.35 \pm 0.22 \mu\text{mol/min/mg}$  of protein, showing a Michaelis–Menten curve (Figure S2A in the Supporting Information). On the contrary, the kinetics of Lipodox was sigmoid (Figure S2B in the Supporting Information), with a higher  $K_{0.5}$  ( $29.1 \pm 1.13 \mu\text{mol/L}$ ) and a slightly lower  $V_{\text{max}}$  ( $8.39 \pm 0.11 \mu\text{mol/min/mg}$  of protein).

We then wondered if, besides reducing its own efflux as well as the efflux of other substrates, Lipodox also inhibited the enzymatic activity of the transporter, and we measured the ATPase activity in Pgp-enriched vesicles from HT29 Pgp<sup>+</sup> cells. While doxorubicin did not affect the rate of ATP hydrolysis, we found

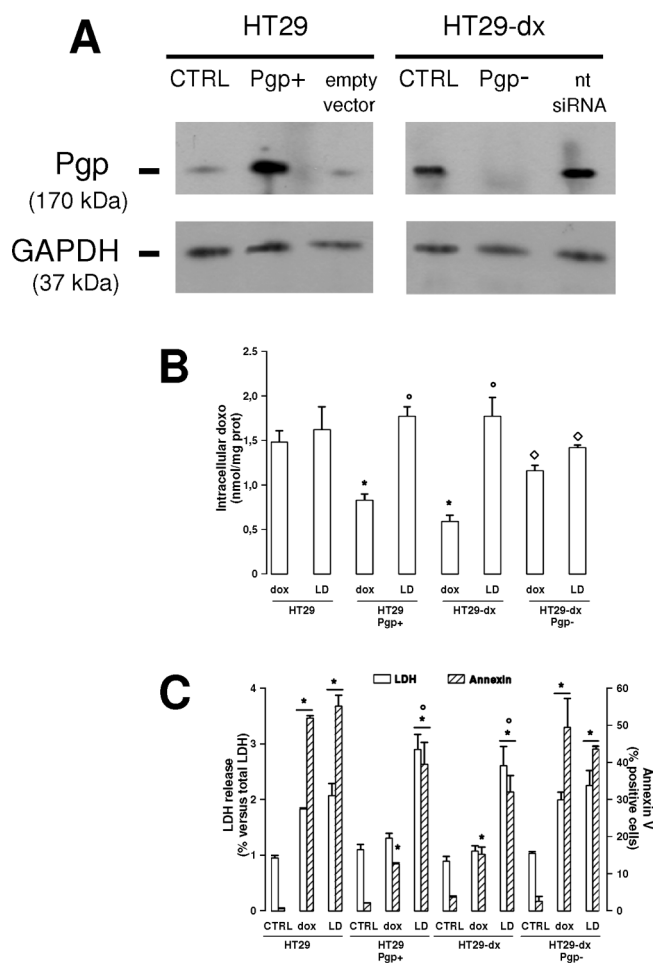


**Figure 4.** Effects of doxorubicin and Lipodox in wild-type HT29 and HT29-dx cells, in Pgp-overexpressing HT29 cells, and in Pgp-silenced HT29-dx cells. An aliquot of wild type HT29 cells was transfected with pCDNA3 vector containing the complete Pgp cDNA to obtain the HT29 Pgp<sup>+</sup> cell population; an aliquot of wild type HT29-dx cells was treated with a specific siRNA for Pgp, to generate the HT29-dx Pgp<sup>-</sup> subline, as reported in Materials and Methods. All cell populations were incubated for 24 h without (CTRL) or with 5  $\mu\text{mol/L}$  doxorubicin (dox) or liposomal doxorubicin (LD) and subjected to the following investigations. (A) Western blot analysis of Pgp after transfection and silencing. As a control of the experimental procedures specificity, an aliquot of HT29 cells was transfected with empty pCDNA3 (empty vector), whereas an aliquot of HT29-dx cells was treated with a nontargeting scrambled siRNA sequence (nt siRNA). The expression of the housekeeping protein GAPDH was measured as a control of equal loading. The results are representative of two similar experiments. (B) The intracellular doxorubicin accumulation was assessed as reported in Materials and Methods. The measurements were performed in triplicate and data are presented as mean  $\pm$  SD ( $n = 3$ ). Vs HT29 dox:  $^*p < 0.005$ . Vs HT29-dx dox:  $^{\circ}p < 0.002$ . LD vs corresponding dox:  $^{\circ}p < 0.002$ . (C) The release of LDH in the cell culture supernatant (open bars) and the positivity for annexin V–FITC (hatched bars) were measured in duplicate as indicated in Materials and Methods. Data are presented as mean  $\pm$  SD ( $n = 3$ ). Vs respective CTRL:  $^*p < 0.005$ . LD vs corresponding dox:  $^{\circ}p < 0.002$ .

that a small inhibition was exerted by high micromolar concentrations of empty liposomes and a stronger reduction by doxorubicin-loaded liposomes (Figure 5D). Thanks to the dual property of reducing its own efflux and the enzymatic efficiency of Pgp, Lipodox displayed a significantly lower  $\text{IC}_{50}$  than

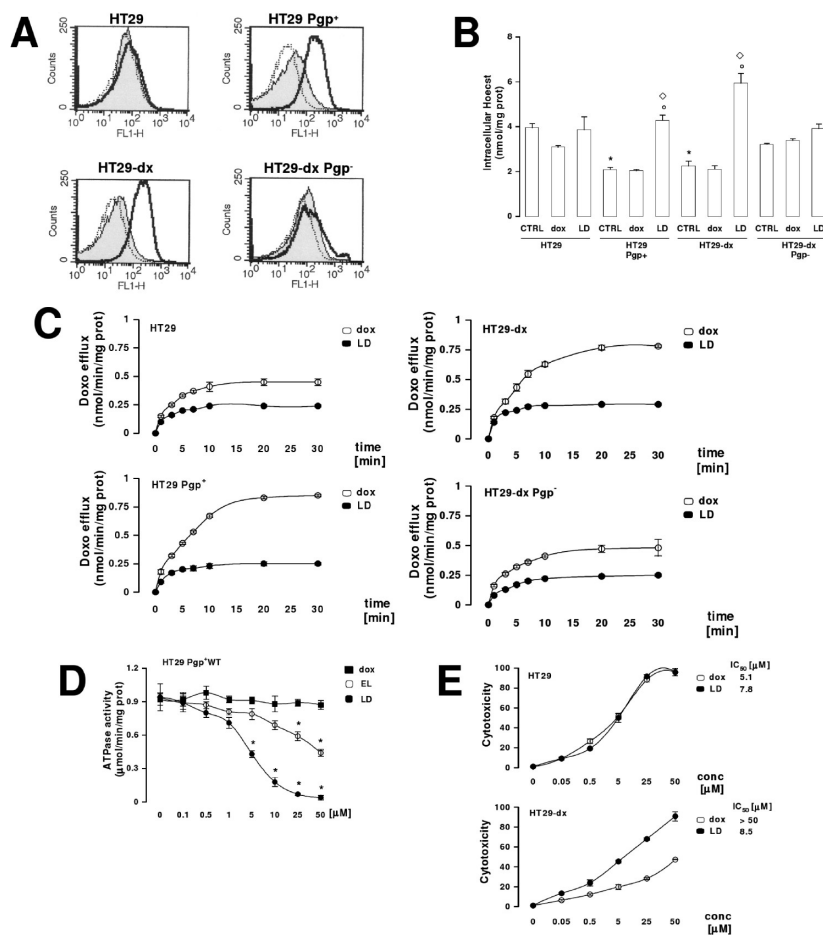


**Figure 5.** Pgp activity in the presence of doxorubicin and Lipodox in wild-type HT29 and HT29-dx cells, in Pgp-overexpressing HT29 cells, and in Pgp-silenced HT29-dx cells. (A) Wild type HT29 cells, HT29 Pgp<sup>+</sup> cells, HT29-dx cells and HT29-dx Pgp<sup>-</sup> cells were incubated for 3 h in fresh medium (CTRL) or with 5 μmol/L doxorubicin (dox) or Lipodox (LD), then washed and maintained for further 20 min at 37 °C in Fresh medium containing rhodamine 123. The intracellular fluorescence of the Pgp substrate rhodamine, inversely related to its efflux, was assessed by flow cytometry analysis (see Materials and Methods) in untreated cells (gray peak), in doxorubicin-incubated cells (dotted line) and in Lipodox-incubated cells (continuous line). The figures shown here are representative of three similar experiments, performed in duplicate. (B) Cells were treated as reported for panel A, then washed and incubated for 15 min at 37 °C in DBPS buffer with Hoechst 33342, lysed and analyzed fluorimetrically for the intracellular content of the dye. Measurements were performed in duplicate and data are presented as mean ± SD (*n* = 3). Vs HT29 CTRL: \**p* < 0.001. Vs HT29 Pgp<sup>+</sup> or HT29-dx CTRL: °*p* < 0.001. LD vs corresponding dox: ◇*p* < 0.002. (C) Cells were incubated for 20 min with 5 μmol/L doxorubicin (dox) or Lipodox (LD), then washed five times and rinsed with 1 mL of PBS; the extracellular amount of doxorubicin was measured fluorimetrically in triplicate immediately after washing (time 0) and at fixed time points up to 30 min, as indicated under Materials and Methods. Data are presented as mean ± SD (*n* = 3). (D) HT29 Pgp<sup>+</sup> cells were lysed, and the Pgp-rich membrane vesicles were isolated; samples were incubated for 30 min at 37 °C with different concentrations of doxorubicin (dox), empty liposomes (EL) or Lipodox (LD); then the ATPase activity was measured as reported under Materials and Methods. Experiments were performed in triplicate, and data are presented as mean ± SD (*n* = 3). Vs respective “0” concentration: \**p* < 0.01. (E) HT29 and HT29-dx were incubated for 24 h with increasing concentrations of doxorubicin (dox) or Lipodox (LD); then the extracellular medium was collected and checked for the extracellular LDH activity, taken as an index of cytotoxicity. Experiments were performed in duplicate, and data are presented as mean ± SD (*n* = 3). IC<sub>50</sub> was calculated as indicated under Materials and Methods.

doxorubicin in drug-resistant cells (Figure 5E). Moreover, differently from doxorubicin, the IC<sub>50</sub> of Lipodox did not differ between HT29 and HT29-dx cells (Figure 5E).

The inhibition of Pgp activity exerted by Lipodox was dose- and time-dependent. At 0.5 μmol/L, a concentration at which its intracellular accumulation remained low and superimposable to free doxorubicin (Figures 2A and 2B), Lipodox did not exert any inhibitory effect on rhodamine efflux (Figure S3A in the Supporting Information) and Hoechst retention (Figure S3B in the Supporting Information). On the contrary, at 5 μmol/L, at which the intracellular accumulation of Lipodox was significantly higher than that of free doxorubicin in drug-resistant cells (Figure 2B),

the Pgp activity was lowered in HT29-dx cells (Figure S3A and S3B in the Supporting Information). Free doxorubicin, at both 0.5 and 5 μmol/L, did not affect the efflux of rhodamine and Hoechst, either in HT29 or in HT29-dx cells (Figure S3A and Figure S3B in the Supporting Information). These experiments suggested that Lipodox must enter and accumulate at a sufficient amount within cells in order to reduce the efflux activity of Pgp. When coincubated with rhodamine, Lipodox was not able to affect the extrusion of rhodamine (Figure S4 in the Supporting Information), whereas it affected the efflux after 3 h (Figure 5A).

In order to increase the delivery of liposomes into cells, we prolonged the incubation times, pretreating HT29 Pgp<sup>+</sup> cells for



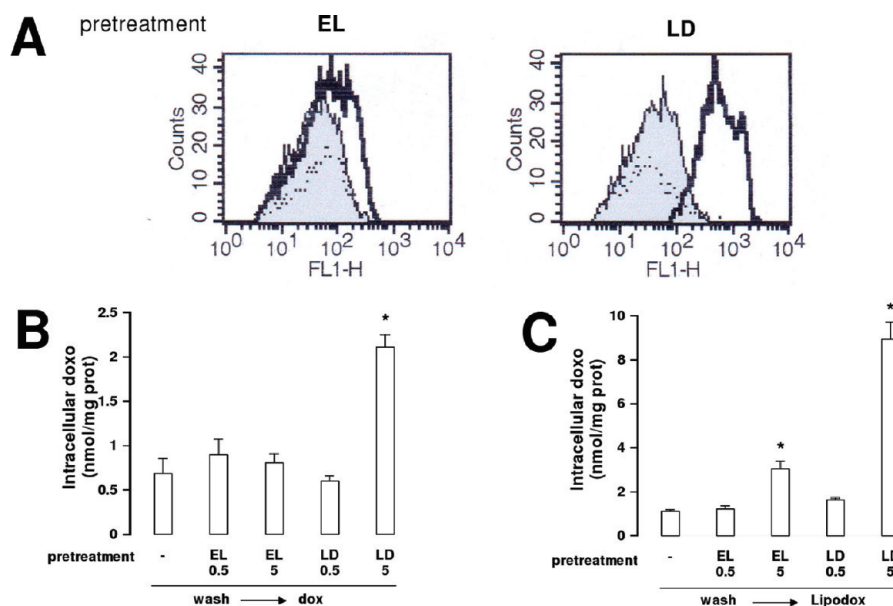


**Figure 6.** Effects of the pretreatment with either empty liposomes or doxorubicin-loaded liposomes on the intracellular retention of rhodamine, doxorubicin or Lipodox. HT29 *Pgp*<sup>+</sup> cells were incubated for 24 h in the absence or in the presence of 0.5 and 5  $\mu$ M/L empty liposomes (EL) or Lipodox (LD), then extensively washed and subjected to the following investigations. (A) Cells were maintained for a further 20 min at 37 °C in Hepes-buffer containing rhodamine 123; then the intracellular fluorescence of the *Pgp*-substrate rhodamine was assessed by flow cytometry analysis (see Materials and Methods) in untreated cells (gray peak), and in cells pretreated with 0.5 (dotted line) or 5  $\mu$ M/L (continuous line) empty liposomes or Lipodox. The figures shown here are representative of three similar experiments, performed in duplicate. Similar results were obtained preincubating the cells for 3 h instead of 24 h (data not shown). (B) Cells were incubated for a further 3 h with 5  $\mu$ M/L doxorubicin, then lysed and analyzed for the intracellular drug content. Measurements were performed in duplicate, and data are presented as mean  $\pm$  SD ( $n = 3$ ). Vs non-pretreated (“–”) cells: \*  $p < 0.002$ . (C) Cells were incubated for 3 h with 5  $\mu$ M/L Lipodox; then the intracellular amount of doxorubicin was measured in duplicate as detailed in Materials and Methods. Data are presented as mean  $\pm$  SD ( $n = 3$ ). Vs non-pretreated (“–”) cells: \*  $p < 0.01$ .

24 h with empty liposomes or Lipodox; then we exposed cells to rhodamine, free doxorubicin or Lipodox, measuring their intracellular accumulation. Again retention of rhodamine (Figure 6A) and doxorubicin (Figure 6B) was increased only by the pretreatment with Lipodox. Surprisingly however the pretreatment with 5  $\mu$ M/L empty liposomes increased the accumulation of a subsequent dose (5  $\mu$ M/L) of Lipodox if compared to cells treated with one dose of 5  $\mu$ M/L Lipodox alone (Figure 6C). This result indicated that also empty liposomes had an effect on *Pgp* (after interacting with cells at a sufficient amount and for a sufficient time), but that they affected the efflux rate only of specific *Pgp* substrates. Also when we pretreated HT29 *Pgp*<sup>+</sup> cells with Lipodox instead of empty liposomes, the accumulation of a second dose of Lipodox was increased (Figure 6C). The accumulation obtained after the sequential treatment with 5  $\mu$ M/L Lipodox plus 5  $\mu$ M/L Lipodox was more than twice the accumulation obtained after 5  $\mu$ M/L empty liposomes plus 5  $\mu$ M/L Lipodox, suggesting that empty liposomes and Lipodox did not display an additive effect. Considering this result and the different kinetics of ATPase inhibition obtained with empty liposomes and Lipodox, we hypothesized that they exert two different but cooperative effects on *Pgp*.

**Anionic Empty Liposomes Affect the Composition of Lipid Rafts and Decrease the Amount of Raft-Associated *Pgp*.** *Pgp* is highly compartmentalized within plasma membrane and is particularly concentrated in detergent-resistant membrane domains like lipid rafts.<sup>26</sup> To investigate whether the empty liposomes effects were due to the targeting of the membrane microenvironment in which *Pgp* works, we extracted and analyzed the lipid rafts from HT29-dx cells treated 24 h with fresh medium, 0.5 or 5  $\mu$ M/L empty liposomes. Empty liposomes

did not change the cholesterol content in lipid rafts (data not shown). The more evident changes in whole membrane fraction were a small increase of phosphatidylcholine and a marked decrease of phosphatidylinositol, that was greater at 5  $\mu$ M/L (Figure 7A); these modifications were observed also in lipid raft extracts (Figure 7B). No changes in the amount of sphingomyelin, the most abundant phospholipid present in lipid rafts, were detected (Figure 7B). On the contrary the fatty acid composition of the microdomains was significantly affected by empty liposome treatment (Table 1). In particular it is possible to observe that empty liposomes induced an increase of palmitate (C16:0), which is the major fatty acid of these phosphatidylethanolamine/phosphatidylcholine/phosphatidylglycerol vesicles. Linolenic acid (C18:2  $\omega$ -6) and arachidonic acid (C20:4  $\omega$ -6) are the major polyunsaturated fatty acids in rafts and were significantly decreased after empty liposome treatment. On the contrary C18:3  $\omega$ -3 fatty acid was increased by liposomes. The other polyunsaturated fatty acids were present in a percentage below 1%. Overall the total  $\omega$ -6 fatty acids were reduced, the ratio  $\omega$ -3/ $\omega$ -6 fatty acids was increased and the ratio polyunsaturated/saturated fatty acids was decreased, indicating an increase of rigidity of rafts. Similar changes in fatty acid composition were detected also in the whole membrane fraction (data not shown).

*Pgp* was clearly detectable in raft extracts (Figure 7C). Interestingly, 5  $\mu$ M/L empty liposomes, a dose that increased the retention of Lipodox (Figure 6C) and modified the composition of lipid rafts (Figure 7B, Table 1), also slightly reduced the amount of raft-associated *Pgp* (Figure 7C).

**Lipodox Interferes with the Binding of Verapamil and Colchicine to *Pgp*.** Beside the indirect effects exerted by

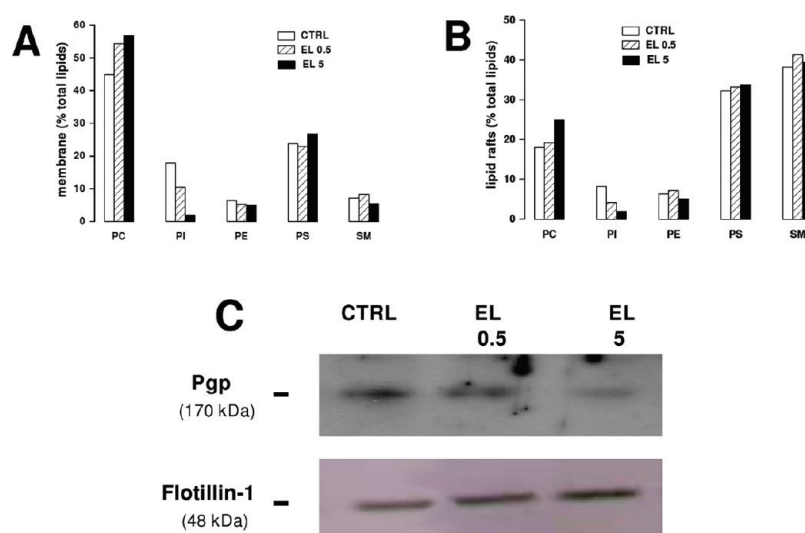


**Figure 7.** Effects of empty liposomes on lipid raft composition and Pgp-amount. HT29-dx cells were grown for 24 h in fresh medium (CTRL) or in a medium containing 0.5 and 5  $\mu\text{mol/L}$  empty liposomes (EL), then lysed and subjected to the extraction of whole membrane and lipid rafts fraction. (A, B) Phospholipids (phosphatidylcholine PC, phosphatidylinositol PI, phosphatidylethanolamine PE, phosphatidylserine PS, sphingomyelin SM) of either whole membrane (panel A) or lipid raft (panel B) fractions were separated by gas chromatography, and the percentages of each phospholipid class, versus the total amount of phospholipids, were calculated from the chromatograms. The histograms are representative of two chromatograms with similar results. (C) Lipid raft extracts were checked for the expression of Pgp by Western blotting, as reported in Materials and Methods. The expression of the flotillin-1 was measured as equal control loading. The results shown here are representative of two similar experiments.

**Table 1.** Percentage of Fatty Acids Contained in Phospholipids Extracted from Lipid Rafts of HT29-dx Cells Treated with Empty Liposomes (0.5 or 5  $\mu\text{mol/L}$  for 24 h) versus Untreated (CTRL) Cells<sup>a</sup>

	CTRL	empty liposomes (%)	
		0.5 $\mu\text{mol/L}$	5 $\mu\text{mol/L}$
C16:0	38.990 $\pm$ 3.2923	41.130 $\pm$ 3.413	41.760 $\pm$ 1.888*
C16:1	5.488 $\pm$ 2.976	5.142 $\pm$ 3.283	4.335 $\pm$ 2.004
C18:0	16.124 $\pm$ 0.951	15.627 $\pm$ 1.295	14.256 $\pm$ 2.825
C18:1	28.438 $\pm$ 4.213	30.901 $\pm$ 2.114	30.743 $\pm$ 1.316
C18:2 $\omega$ -6	3.8406 $\pm$ 1.359	2.025 $\pm$ 0.113*	2.109 $\pm$ 0.494*
C18:3 $\omega$ -3	1.366 $\pm$ 1.312	2.247 $\pm$ 1.958	2.527 $\pm$ 1.563
C18:3 $\omega$ -6	0.169 $\pm$ 0.197	0.132 $\pm$ 0.102	0.432 $\pm$ 0.438
C20:3 $\omega$ -6	0.872 $\pm$ 0.567	0.468 $\pm$ 0.460*	0.483 $\pm$ 0.094*
C20:4 $\omega$ -6	2.754 $\pm$ 0.958	1.124 $\pm$ 1.062*	2.489 $\pm$ 0.927
C20:5 $\omega$ -3	0.447 $\pm$ 0.404	0.236 $\pm$ 0.168	0.143 $\pm$ 0.124
C22:5 $\omega$ -3	0.739 $\pm$ 0.835	1.337 $\pm$ 0.815	0.632 $\pm$ 0.325
C22:6 $\omega$ -3	0.772 $\pm$ 0.551	0.432 $\pm$ 0.254	0.183 $\pm$ 0.317
saturated	55.114 $\pm$ 3.792	56.757 $\pm$ 2.166	56.016 $\pm$ 1.200
monounsaturated	33.926 $\pm$ 4.002	36.043 $\pm$ 2.232	35.078 $\pm$ 1.669
polyunsaturated	10.959 $\pm$ 3.240	7.199 $\pm$ 2.324	8.906 $\pm$ 0.817
total $\omega$ -6	7.635 $\pm$ 2.458	3.616 $\pm$ 0.704*	5.353 $\pm$ 0.971*
total $\omega$ -3	2.877 $\pm$ 1.664	3.583 $\pm$ 1.819	3.410 $\pm$ 1.307
polyunsaturated/ saturated	0.216 $\pm$ 0.062	0.129 $\pm$ 0.081*	0.159 $\pm$ 0.014*

<sup>a</sup>Results are expressed as percentage of total fatty acids  $\pm$  SD. Significance: \* $p < 0.05$ .

liposomal shell, we wondered whether doxorubicin-loaded liposomes exerted their inhibition on Pgp by directly interacting with the transporter and, if so, with which Pgp domain they may

interact. To this aim, we examined what happened to Lipodox retention in the presence of known Pgp inhibitors, such as verapamil and cyclosporin A, and of a substrate like colchicine. As expected, verapamil and cyclosporin A significantly increased the intracellular content of doxorubicin in HT29 *Pgp*<sup>+</sup> cells (Figure 8A), whereas the coinubation with colchicine did not modify the anthracycline accumulation at any concentration tested (Figure 8C). Lipodox accumulation was higher than that of free doxorubicin in HT29 *Pgp*<sup>+</sup> cells, but no further enhancement was observed in the presence of verapamil and cyclosporin A (Figure 8A). Surprisingly the addition of colchicine significantly reduced the retention of 5  $\mu\text{mol/L}$  Lipodox, although the effect of colchicine was overcome by increasing amounts of Lipodox (Figure 8C). Superimposable results were obtained in native HT29-dx cells (data not shown).

Lipodox markedly inhibited the binding of verapamil to Pgp, reproducing the same displacement exerted by cold verapamil (Figure 8B). When we measured the verapamil-induced ATPase activity, we observed that Lipodox dose-dependently reduced the  $K_m$  of verapamil (Figure S5C,D in the Supporting Information), mimicking the inhibition exerted by a classical competitive inhibitor like cyclosporin A (Figure S5A,B in the Supporting Information). Lipodox also reduced the binding of colchicine to Pgp, but in this case the binding profile differed from that of cold colchicine (Figure 8D), indicating that the liposome-derived drug did not interact with the transporter exactly like colchicine. In parallel Lipodox decreased the small increase in ATPase activity elicited by colchicine (Figure S5E in the Supporting Information), with a kinetics suggestive of a negative allosteric effect. Free doxorubicin did not affect either the binding of verapamil and colchicine (Figure 8B and 8D) or the ATPase activity of Pgp in the presence of these compounds (Figure S5C–E in the Supporting Information).

These results led us to hypothesize that Lipodox could directly interact with Pgp on a putative site near or coincident with the verapamil- and the colchicine-binding site.

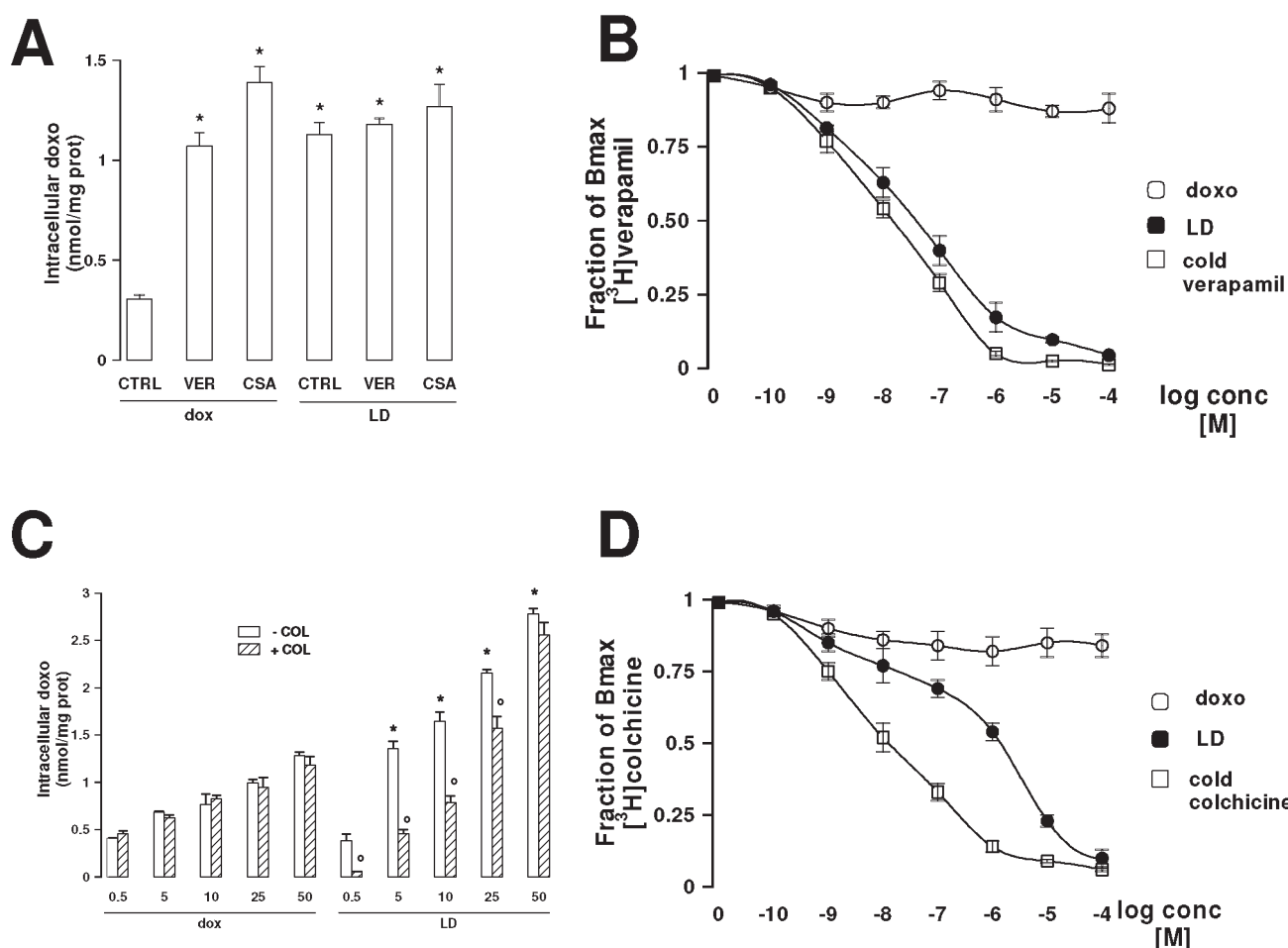


**Figure 8.** Effects of the coinubation of Lipodox with different inhibitors and substrates of Pgp. (A) HT29 Pgp<sup>+</sup> cells were grown for 24 h in the presence of 5  $\mu\text{mol/L}$  doxorubicin (doxo) or Lipodox (LD), alone (CTRL) or in coinubation with 10  $\mu\text{mol/L}$  verapamil (VER) or 10  $\mu\text{mol/L}$  cyclosporin A (CSA). The intracellular doxorubicin amount was measured as reported under Materials and Methods. Data are presented as mean  $\pm$  SD ( $n = 4$ ). Vs CTRL doxo:  $*p < 0.001$ . (B) The binding assay of [ $^3\text{H}$ ]verapamil, in the presence of increasing concentrations of doxorubicin (doxo), Lipodox (LD) or cold verapamil was performed on Pgp-rich membrane vesicles, isolated from HT29 Pgp<sup>+</sup> cells, as reported under Materials and Methods. Experiments were conducted in quadruplicate and data are presented as mean  $\pm$  SD ( $n = 3$ ). (C) HT29 Pgp<sup>+</sup> cells were grown for 24 h in the presence of 0.5–50  $\mu\text{mol/L}$  doxorubicin (doxo) or Lipodox (LD), in the absence or presence of 100  $\mu\text{mol/L}$  colchicine (COL); then the intracellular doxorubicin amount was measured fluorimetrically. Data are presented as mean  $\pm$  SD ( $n = 4$ ). Vs CTRL doxo:  $*p < 0.001$ . Vs LD–COL:  $*p < 0.001$ . (D) The binding assay of [ $^3\text{H}$ ]colchicine, in the presence of increasing concentrations of doxorubicin (doxo), Lipodox (LD) or cold colchicine was performed on Pgp-rich membrane vesicles isolated from HT29 Pgp<sup>+</sup> cells, as reported. Experiments were made in quadruplicate, and data are presented as mean  $\pm$  SD ( $n = 3$ ).

**Glycine 185 of Pgp Is Essential for the Inhibitory Properties of Lipodox.** Glycine 185 plays a pivotal role in modulating the ATPase activity of Pgp and the drug efflux.<sup>27,28</sup> The substitution of glycine with valine (G185 V mutation) has been identified for the first time in cells selected for the resistance to colchicine;<sup>29</sup> the mutated protein revealed an altered binding and affinity for colchicine, verapamil and cyclosporin A.<sup>30</sup> Starting from this observation, and considering the results of binding assays, we wondered if glycine 185 was a critical site also for the interaction of Lipodox with Pgp. By site-directed mutagenesis, we produced the pCDNA3 expression vector containing the G185 V Pgp cDNA. As shown in Figure 9A, the G185 V Pgp was expressed in HT29 cells at the same level of the wild type Pgp (contained in the HT29 Pgp<sup>+</sup> cell population). In cells transfected with both wild-type and mutated vector, the Pgp levels were higher than in parental HT29 cells (Figure 9A). The overexpression of wild type and G185 V Pgp resulted in a reduced accumulation of doxorubicin (Figure 9B) and in an increased efflux of rhodamine

(Figure 9C), indicating that mutated Pgp is as functional as wild-type Pgp, in front of the efflux of doxorubicin and rhodamine. HT29 Pgp<sup>+</sup> cells treated with Lipodox showed an enhanced accumulation of the drug, in comparison with free doxorubicin (Figure 9B) and a lower activity of Pgp (Figure 9C). On the contrary when Pgp contained the G185 V, the content of Lipodox was significantly lower than in cells containing the wild-type Pgp and did not differ from the content of free doxorubicin (Figure 9B). Lipodox also lost the ability to reduce the efflux of rhodamine through G185 V Pgp (Figure 9C) and to decrease the Pgp ATPase activity, except at the concentrations of 25 and 50  $\mu\text{mol/L}$  (Figure 9D). Interestingly the inhibition of ATPase activity achieved by Lipodox on G185 V Pgp resembled that exerted by empty liposomes on wild-type Pgp (Figure 5D).

## DISCUSSION

In recent years the synthesis of modified formulations of doxorubicin, such as albumin-conjugated,<sup>31</sup> antibody-coupled<sup>32</sup>



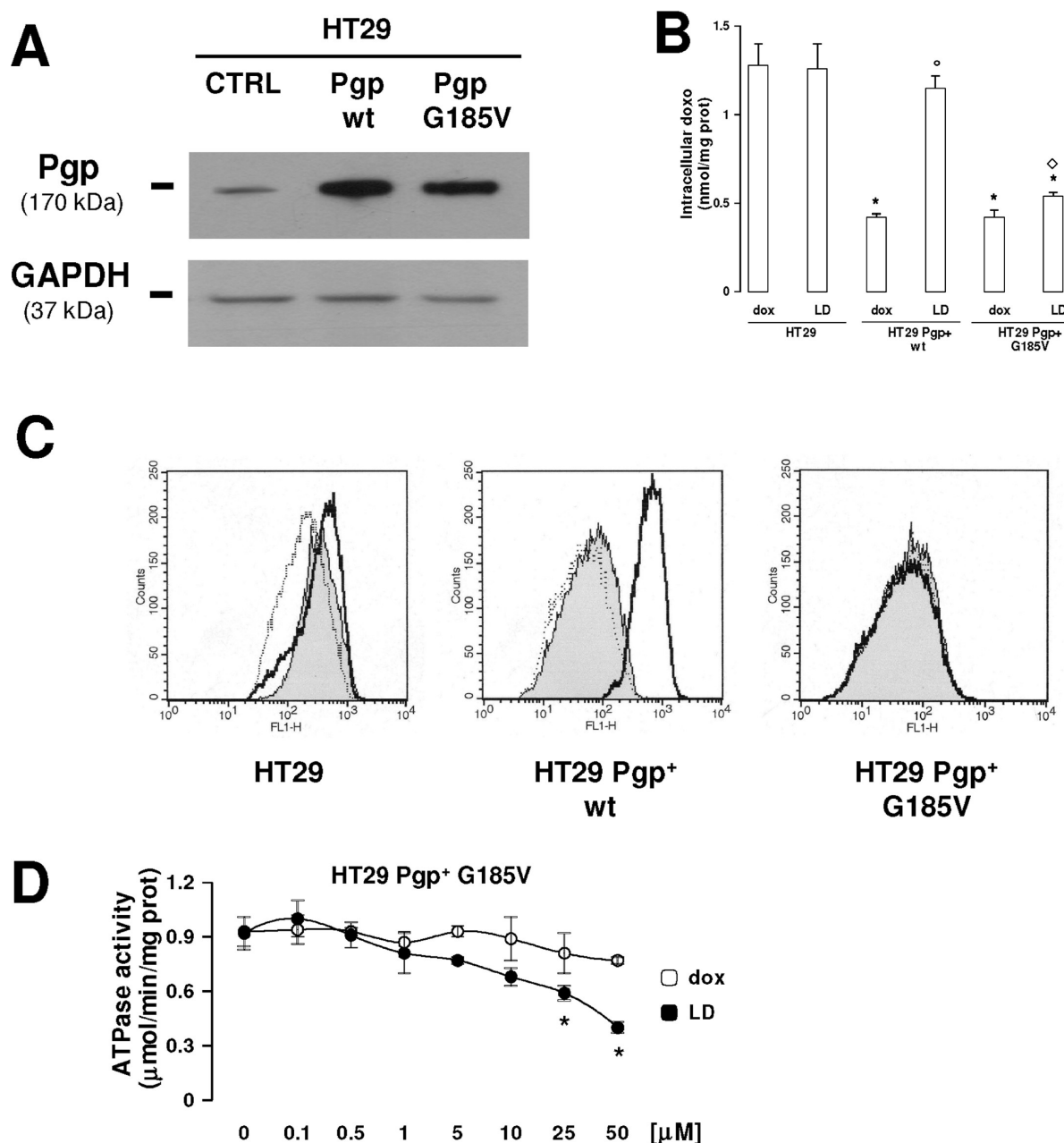


**Figure 9.** Effects of the G185 V mutation on Lipodox content and modulation of Pgp activity. (A) Parental HT29 cells (CTRL) and HT29 cells transfected with pCDNA3 vector, respectively containing the wild-type (Pgp wt) or the mutated (Pgp G185 V) sequence, were checked for the expression of Pgp by Western blotting, as reported in Materials and Methods. The expression of the housekeeping protein GAPDH was measured as equal control loading. The results shown here are representative of two similar experiments. (B) The cell populations of panel A were incubated for 24 h in the absence (CTRL) or presence of 5  $\mu\text{mol/L}$  doxorubicin (dox) or Lipodox (LD); then the doxorubicin retention was detected fluorimetrically in duplicate. Data are presented as mean  $\pm$  SD ( $n = 3$ ). Vs HT29 dox:  $*p < 0.002$ . Vs HT29 Pgp<sup>+</sup> wt dox:  $^{\circ}p < 0.005$ . HT29 Pgp<sup>+</sup> G185 V vs the corresponding HT29 Pgp<sup>+</sup> wt:  $^{\diamond}p < 0.002$ . (C) Parental HT29 cells, HT29 Pgp<sup>+</sup> wt and HT29 Pgp<sup>+</sup> G185 V were incubated for 3 h in fresh medium (gray peak) or with 5  $\mu\text{mol/L}$  doxorubicin (dotted line) or Lipodox (continuous line); then the activity of Pgp, measured as the rate of efflux of rhodamine, was evaluated by flow cytometry analysis (see Materials and Methods). The figures shown here are representative of three similar experiments, performed in duplicate. (D) HT29 Pgp<sup>+</sup> G185 V cells were lysed and the Pgp-containing membrane vesicles were isolated to measure the ATPase activity in the presence of increasing concentrations of doxorubicin (dox) or Lipodox (LD), as reported under Materials and Methods. Experiments were performed in triplicate, and data are presented as mean  $\pm$  SD ( $n = 3$ ). Vs respective "0" concentration:  $*p < 0.005$ .

or liposomal<sup>12,14,22</sup> doxorubicin, has been proposed as a useful tool, which maximizes the toxic effects against the tumors, with a relative sparing of toxicity on heart and non-transformed tissues. Interestingly liposomal drugs accumulate preferentially within tumor bulks, probably because of their leakage through the

fenestration of tumoral vessels, which are less present in the vasculature of non-transformed tissues.<sup>10</sup> A particular efficacy of liposomes in tumors resistant to conventional chemotherapy has been reported,<sup>10,16</sup> but the mechanism is still a matter of debate: for instance it is not clear if the benefits of the

liposome-encapsulated drugs derive from the carrier only or from the whole formulation (liposomes loaded with the drug) and if a direct interaction with Pgp, which is responsible for the efflux of most anticancer agents, is at the basis of the advantages of liposomal drugs.

To investigate this issue, we produced anionic liposomes loaded with doxorubicin (Lipodox) and compared their effects with those of free doxorubicin in human drug-sensitive colon cancer HT29 cells and in drug-resistant HT29-dx cells. We did not detect any difference between doxorubicin and Lipodox in intracellular accumulation and cytotoxicity in sensitive cells; on the contrary, in resistant cells Lipodox was significantly more effective than the free drug, when used at 5–25  $\mu\text{mol/L}$ . Notably, at 5  $\mu\text{mol/L}$  Lipodox was retained in resistant cells at the same extent than in sensitive cells, whereas the accumulation of free doxorubicin in HT29-dx cells was significantly lower even at the higher concentrations. It has been demonstrated that doxorubicin readily enters cells by passive diffusion within a few minutes and is pumped out by active transport through ABC transporters.<sup>33</sup> In our experimental conditions the difference between doxorubicin and Lipodox accumulation was detected also after brief incubation times (1 or 3 h) and progressively increased at each time point in HT29-dx cells. Such a difference at early time points appears compatible with the fast kinetics of doxorubicin efflux through Pgp and MRPs, which determine a  $t_{1/2}$  of the doxorubicin intracellular content of about 2 min when the drug is in the micromolar range.<sup>33</sup> We may suppose that doxorubicin and Lipodox enter the cells and are readily pumped out by membrane transporters as a function of time, but the kinetics of efflux is different between the free drug and the liposome-encapsulated drug. A previous work reported that free doxorubicin accumulates in the nucleus in sensitive breast cancer cells and is sequestered in the cytosol in doxorubicin-resistant ones, whereas the liposomal envelope makes the drug able to reach the nucleus also in resistant tumors.<sup>17</sup> In our experimental model Lipodox accumulates in the nucleus in HT29 as well as in HT29-dx cells, excluding a different cytosolic sequestration between sensitive and resistant cells. HT29 cells have very low levels of ABC transporters, whereas HT29-dx cells have abundant amounts of Pgp.<sup>20</sup> Moreover in all tumor cells overexpressing Pgp that we checked, Lipodox accumulated significantly more than doxorubicin, whereas in sensitive cells, with a low or undetectable level of Pgp, the difference between liposome-entrapped and free drug was nearly reduced to zero. Although we cannot exclude that an increased uptake may contribute to the preferential accumulation of Lipodox in drug-resistant cells, as it occurs with cationic liposomal paclitaxel in NIH-3T3 cells overexpressing Pgp,<sup>34</sup> the greater efficacy of Lipodox toward doxorubicin appeared strictly correlated with the expression levels of Pgp. We could hypothesize that in the absence of Pgp free doxorubicin and Lipodox are retained within cells to the same extent and exert the same toxicity; in cells overexpressing Pgp, doxorubicin is pumped out, whereas Lipodox is less extruded and progressively accumulates within cells, reaching toxic concentrations.

Interestingly, when transfected with Pgp full cDNA, HT29 cells became similar to HT29-dx cells as far as accumulation and toxic effects of doxorubicin and Lipodox were concerned; on the contrary, when deprived of Pgp by selective silencing, HT29-dx cells showed no preferential accumulation of either drug formulation. Our data are in keeping with other works, showing a greater efficacy of liposome-encapsulated drugs in resistant cancer cells.<sup>13–15</sup> On the other hand our results do not suggest

significant advantages in using Lipodox instead of doxorubicin in sensitive cells with low levels of Pgp, as suggested by the similar  $\text{IC}_{50}$  between doxorubicin and Lipodox in HT29 cells, in contrast to the great difference of  $\text{IC}_{50}$  observed in HT29-dx cells.

These data also confirm that Pgp is critical for the efflux of Lipodox, and that both doxorubicin and Lipodox could be transported by Pgp, although with different kinetics or affinity. If we compare the efflux of doxorubicin from cells treated with either free drug or Lipodox, the latter was significantly less extruded than free doxorubicin. Moreover the efflux of Lipodox remained low in all cell populations of Figure 5C, regardless of the Pgp expression level, whereas free doxorubicin was more actively pumped out in HT29-dx and in HT29 Pgp<sup>+</sup> cells. The study of kinetic parameters indicated that the Pgp activity followed a Michaelis–Menten curve for doxorubicin, and a sigmoid curve for Lipodox, which had a higher  $K_{0.5}$  value than the free drug. These results led to the hypothesis that Lipodox has a poorer affinity for Pgp than doxorubicin and can act as a negative allosteric modulator. Also the  $V_{\text{max}}$  of Lipodox was slightly lower, suggesting that cells exposed to Lipodox might also have a reduced amount of active Pgp.

The effects exerted by liposome-encapsulated drugs on Pgp activity are still controversial: for instance the antitumor effect of anionic liposomes, which are readily internalized by drug-resistant cells, has been attributed to the direct binding of Pgp,<sup>35</sup> which subsequently would slow down its activity. However, a similar antitumor efficacy has been displayed also by neutral liposomes, which hardly fuse with the plasma membrane and can only provide a higher diffusion of the drug remaining in the extracellular environment.<sup>35</sup> To clarify whether Lipodox directly affected the function of Pgp, we measured the efflux of rhodamine 123 and Hoechst 33342, well-known substrates of this transporter,<sup>2</sup> in cells exposed to either doxorubicin or Lipodox. In cells overexpressing Pgp, free doxorubicin did not change the rhodamine efflux or the Hoechst accumulation compared to untreated cells, suggesting that, in the presence of the free anthracycline, the activity of Pgp was not modified. Instead, Lipodox markedly increased the intracellular accumulation of rhodamine and Hoechst in Pgp-rich cells (HT29-dx and HT29 Pgp<sup>+</sup> cells), thus indicating a reduced activity of the pump. This effect was not observed in Pgp-poor cells (HT29 cells and HT29-dx Pgp<sup>-</sup> cells), where the intracellular content of rhodamine and Hoechst remained high and not modified by either doxorubicin or Lipodox. Interestingly it has been recently reported that in Pgp-overexpressing MCF-7 cells the liposomes may alter *per se* the Pgp activity, since the efflux of liposomal rhodamine was significantly lower than the efflux of the free dye.<sup>36</sup> In that experimental model the presence of cholesterol and polyethylene glycol, two components present in our anionic liposomes, was a critical factor for the interaction of liposomes with Pgp.<sup>36</sup> In our Pgp-rich membrane extracts, the Lipodox, differently from free doxorubicin, exerted a direct inhibition on the Pgp ATPase activity. ATP binding and subsequent hydrolysis is a crucial step to trigger a conformational reorganization of the pump, opening a central pore that allows the hydrophobic drugs to be transported outside directly from the lipid bilayer.<sup>37</sup> It is conceivable that the impaired ATP hydrolysis exerted by Lipodox would result in an impaired extrusion of substrates. Lipodox can be more effective in cells overexpressing Pgp not only because it is poorly transported by the pump but also because it impairs the ATPase catalytic cycle. By doing so, it increases its own accumulation with a sort of feed-forward mechanism.

Free doxorubicin did not significantly affect the activity of Pgp, as occurs with daunorubicin and epirubicin.<sup>38</sup> On the other hand, empty liposomes reduced the enzymatic activity of Pgp in membrane extracts, but only at high micromolar concentrations. It has been suggested that compounds inhibiting the ATPase activity with an  $EC_{50}$  around 1  $\mu\text{mol/L}$  act by specifically interacting with Pgp, whereas an  $EC_{50}$  between 10 and 100  $\mu\text{mol/L}$  is indicative of an indirect effect on the transporter.<sup>38</sup> The inhibition kinetics of ATPase activity had an  $EC_{50}$  of 5  $\mu\text{mol/L}$  for Lipodox and around 50  $\mu\text{mol/L}$  for empty liposomes. Thus, it is likely that Lipodox and empty liposomes exert two different kinds of inhibition on Pgp.

When we coincubated doxorubicin and empty liposomes, without loading the drug inside the liposomes, the intracellular accumulation of the anthracycline was superimposable to that of doxorubicin alone and was lower than in the presence of Lipodox. Moreover empty liposomes did not affect the activity of Pgp in terms of rhodamine and doxorubicin efflux, whereas doxorubicin-loaded liposomes did. Unexpectedly, however, when incubated for 24 h at 5  $\mu\text{mol/L}$ , empty liposomes enhanced the accumulation of Lipodox, suggesting that an effect of liposomal shell *per se* could be detectable when empty liposomes are allowed to interact with cells at a sufficient amount and for a sufficient time. Moreover such an effect was not exerted on all the Pgp substrates. Being weak inhibitors of Pgp, it is not unreasonable to suppose that an empty liposome effect becomes evident only at high concentrations or for specific Pgp substrates, for instance for the substrates, like Lipodox, that are poorly transported by Pgp and for which a small inhibition of the transporter easily results in a significant increase of intracellular retention.

Similarly to empty liposomes, also the effects of Lipodox were time- and dose-dependent, but became clear at lower concentrations and after shorter times: the activity of Pgp was decreased after 3 and 24 h as a function of Lipodox amounts and was obtained at a concentration (5  $\mu\text{mol/L}$ ) at which the drug was significantly accumulated within the cells. On the contrary at 0.5  $\mu\text{mol/L}$ , when the amount of doxorubicin carried by Lipodox was low and superimposable to that of doxorubicin alone, Lipodox did not modify the efflux of rhodamine and Hoechst in HT29-dx cells. After shorter time-points, i.e. when coincubated for 20 min with rhodamine, Lipodox did not modify the dye efflux. This result may be interpreted as an absence of competition between Lipodox and rhodamine at the Pgp level. We must also consider that after 20 min the amount of intracellular Lipodox is very low ( $0.147 \pm 0.005$  nmol/mg of protein, corresponding to 0.103  $\mu\text{mol/L}$ ) compared with the amount of Lipodox (5  $\mu\text{mol/L}$ ) present on the extracellular side at  $t_0$ . After 3 and 24 h Lipodox accumulated within HT29-dx cells at a higher amount, superimposable to that observed in HT29 cells, and was able to reduce the efflux of rhodamine. We deduced that Lipodox did not affect the activity of Pgp when present on the extracellular side of the transporter, but inhibited it when accumulated at a sufficient amount on the cytosolic side of the pump.

In order to discriminate the effects of empty liposomes *per se* from the effects of doxorubicin-loaded liposomes, we focused on the membrane microenvironment in which Pgp works. Being an integral transporter, Pgp is embedded in the phospholipid bilayer, and small differences in the plasma membrane composition deeply affect its activity.<sup>39</sup> Since the protein is particularly concentrated in the lipid rafts,<sup>26</sup> we wondered whether the lipid addition from liposomal shell might alter the chemical

composition and properties of these membrane domains. In both whole membrane and lipid raft extracts, liposomes increased the amount of phosphatidylcholine, and decreased the amount of phosphatidylinositol. Phosphatidylcholine can be delivered by liposomes themselves, wherein it is contained. As to the decrease of phosphatidylinositol, this could be due to a dilution effect or to an accelerated turnover. Such variations in phospholipids composition may be sufficient to alter the physicochemical properties of membrane bilayer and then Pgp activity.

Furthermore, empty liposomes changed the fatty acid compositions of phospholipids extracted from lipid rafts, e.g. decreasing the amount of polyunsaturated fatty acids and increasing the ratio  $\omega$ -3/ $\omega$ -6 fatty acids. Since the liposomes used in this work contained only saturated fatty acids, these modifications are not the consequence of the fusion between liposomal shell and lipid rafts, but should rather be the result of a fatty acid exchange process, that followed the addition of liposomes. Such changes may reduce membrane fluidity and impair protein signal transduction related to the hydrolysis of phospholipids containing polyunsaturated fatty acids. Moreover the changes in lipid composition of rafts can elicit some conformational changes in Pgp structure and activity; finally empty liposomes dose-dependently reduced the amount of Pgp present in lipid rafts.

In HT29-dx cells the protein content of lipid rafts was very low compared with the total amount of cell proteins, but 5  $\mu\text{g}$  of lipid raft proteins was sufficient to detect Pgp in Western blot experiments, where the same protein was detectable with at least 30  $\mu\text{g}$  of proteins from whole cell lysates. This observation is indicative of a high concentration of Pgp in lipid rafts of HT29-dx cells; for this reason, also a small reduction of the amount of Pgp in rafts, as that elicited by 5  $\mu\text{mol/L}$  empty liposomes, may produce great consequences on the extrusion of substrates. Such a reduction of the enzyme amount may explain the decrease in ATPase activity caused by liposomal shell *per se*. Manipulations of lipid raft composition have been associated with a decreased activity of Pgp and sometimes with a shift toward the soluble fraction.<sup>40,41</sup> Few studies indicate that monoglycerides or lipidic excipients may interfere in Pgp activity decreasing its expression.<sup>42</sup> However this is the first time that a similar effect is reported in drug-resistant tumor cells treated with liposomes.

Besides this indirect effect exerted by liposomal shell on the membrane microenvironment surrounding Pgp, the direct inhibitory effect of doxorubicin-loaded liposomes on Pgp activity seems to imply also a direct interaction with the transporter. This hypothesis arises from previous works reporting that liposomes interfere with the binding of vincristine in cells overexpressing Pgp.<sup>18,19</sup> We thus examined what happened to Lipodox retention in the presence of known Pgp inhibitors and substrates, like verapamil, cyclosporin A and colchicine.

The intracellular accumulation of liposome-encapsulated paclitaxel is enhanced by verapamil, leading to the hypothesis that the nanoparticles are subjected to the efflux through Pgp:<sup>34</sup> the liposomes employed in this study were cationic or neutral ones, whereas in our work we used anionic liposomes. This difference could explain why we did not detect any enhancement of Lipodox retention in the presence of verapamil, which instead increased the accumulation of doxorubicin. Interestingly, a similar pattern was displayed in the presence of another competitive inhibitor of Pgp, like cyclosporin A. When Lipodox was present, verapamil and cyclosporin A were devoid of effects, as if they competed with the liposomal drug for the interaction with Pgp. Anthracyclines and verapamil do not bind at the same site,<sup>43</sup>



but they may reciprocally impair their transport through Pgp, modifying allosterically the pump activity.<sup>25</sup> Being a larger molecule than verapamil, cyclosporin A binds on a different site and induces a conformational change different from verapamil.<sup>44</sup> This situation is compatible with the complex structure of Pgp, which has multiple substrates and modulator-binding sites.<sup>44</sup> Our binding experiments revealed that the addition of Lipodox markedly affected the binding of verapamil and, like cold verapamil, displaced the labeled verapamil, suggesting that Lipodox may interact with the verapamil binding site. The competitive relationship between Lipodox and verapamil was confirmed by the effect on the catalytic activity. Verapamil is known to increase the ATPase activity of Pgp;<sup>25</sup> Lipodox reduced the verapamil-stimulated ATPase activity and increased the  $K_m$  of verapamil, without changing the  $V_{max}$ , as well as the competitive inhibitor cyclosporin A did.

In our experimental conditions colchicine did not affect the intracellular retention of doxorubicin, but drastically reduced the accumulation of Lipodox. Such a reduction was partially reversed by increasing the concentrations of Lipodox. Considering these results, we hypothesized that Lipodox may interact also with the colchicine binding site on Pgp. However, in this case the displacement of labeled colchicine exerted by Lipodox differed from that of cold colchicine, suggesting that Lipodox may not bind to the same site of colchicine. Lipodox binding could instead induce a conformational change which is poorly compatible with the binding of colchicine, therefore acting with an allosteric mechanism. This behavior is common to other lipophilic modulators of Pgp, like the lipid solvents Tween-80 and Cremophor, that inhibit the binding of daunorubicin to Pgp, not by a direct competition, but altering the conformation of the protein in a way that disturbs the binding of other drugs.<sup>45</sup> The kinetic profile of ATPase activity measured when colchicine was coincubated with Lipodox supports the hypothesis that Lipodox acts as a negative modulator of the enzyme versus colchicine. It has been already reported that the same compound can contemporarily act as competitive, noncompetitive or allosteric inhibitor on the binding of other substrates to Pgp, because of the abundance of the drug-binding sites and of the reciprocal modulation existing between each of them.<sup>7</sup> Besides the potential change in Pgp conformation induced by a direct interaction of Lipodox, we also must consider that the change in membrane microenvironment exerted by liposomal shell can affect as well the conformational of Pgp, impairing the binding of other substrates.

The results of the binding experiment also constitute an indirect proof that the critical site for the effects of Lipodox on Pgp should map in a region that is physiologically involved in the binding of verapamil and/or colchicine.

The amino acid at position 185 on Pgp protein is critical for the transport of colchicine; the substitution of glycine, present in wild-type Pgp, with valine has been identified in colchicine-resistant cells, because it allows a faster efflux of the drug.<sup>30</sup> Interestingly the G185 V substitution also affects the binding and efflux of verapamil and cyclosporin A<sup>30</sup> and induces a moderate increase of the resistance to doxorubicin.<sup>46,47</sup> Since the residue 185 is contained in a site common for binding and/or transport of verapamil and colchicine, two of the substrates with which Lipodox interferes, we compared the HT29 Pgp<sup>+</sup> cells, which expressed the wild-type *mdr1* gene, with HT29 cells overexpressing the G185 V mutated Pgp. The latter cell population accumulated significantly less doxorubicin and rhodamine than the parental HT29 cells, suggesting that the mutated protein is

active as efflux pump like the wild-type. However Lipodox was not more accumulated compared to free doxorubicin, did not lower the transport of rhodamine in HT29 G185 V Pgp<sup>+</sup> cells and did not decrease the ATPase activity, except at very high concentrations. Interestingly, the profile of ATPase inhibition exerted by Lipodox on G185 V Pgp<sup>+</sup> cells reproduced the one elicited by empty liposomes in HT29 Pgp<sup>+</sup> cells. In the light of these results we hypothesized that Lipodox exerts its inhibitory effect on Pgp by interacting with a domain located near glycine 185, in the absence of which it could not interact with the transporter, as it did with the wild-type Pgp. The indirect effects exerted by liposomal shell, i.e. the change in lipid rafts composition and Pgp localization, are probably conserved also in G185 V Pgp<sup>+</sup> cells, as indicated by the inhibition curve of ATPase activity; on the contrary the direct inhibitory effect exerted by Lipodox was lost. Amino acid 185 is in the first cytosolic loop between the second and the third transmembrane helix of Pgp<sup>28</sup> and plays an important role in transmitting the conformational changes induced by the drugs binding to the catalytic site.<sup>27</sup> Photoaffinity labeling studies revealed a drug-binding site on the cytosolic side and a drug-releasing site near the transmembrane region of Pgp.<sup>46</sup> Residue 185 is part of a domain which binds several drugs before their release outside the cells: the mutation of glycine 185 may hamper such a release and favor instead the leakage of the drug toward the cytosol.<sup>46</sup> Indeed the G185 V mutation changes the  $K_m$  for colchicine and the number of its binding sites on Pgp,<sup>47</sup> resulting in its enhanced efflux.<sup>46</sup> We cannot exclude that an analogous event occurs also for Lipodox.

It is difficult to conceive that such a big structure like a liposome directly binds one amino acid on Pgp; we believe instead that, after entering within the cells, the doxorubicin previously contained in the liposome core is released, maybe bound with some lipid moiety derived from the liposomal envelope. It has been documented that cardiolipin present in liposomes can complex free doxorubicin, generating a new lipid-associated drug;<sup>19</sup> we cannot exclude that a lipid-complexed doxorubicin is the real inhibitor of Pgp. Having a chemical structure different from free doxorubicin, such a drug should display a different pattern of binding sites on Pgp and a different kinetics of extrusion. The chemical moiety of glycine grants a high degree of flexibility, whereas the lateral chain of valine imposes limitations to the number of the possible tridimensional conformations: it has been demonstrated that the substitution of glycine with valine allows the transition status to be reached with a lower energy of activation, facilitating the catalytic cycle and the efflux of drugs like colchicine and doxorubicin.<sup>27</sup> The substitution glycine to valine could alter as well the conformation of the binding site for the liposomal-derived doxorubicin, impairing its interaction with the pump and reducing its effect as Pgp inhibitor.

In summary our work demonstrates that Lipodox is an inhibitor of Pgp, explaining why it is effective in aggressive and chemoresistant tumors and suggesting that the benefit of Lipodox could be considered as the sum of two distinct mechanisms (Figure 10): (1) an indirect effect, due to the liposomal shell, that changes chemical composition and properties of the membrane microenvironment, impairing the activity and localization of Pgp; (2) a direct effect, due to the interaction of the liposome-derived doxorubicin with Pgp itself, that becomes less prone to recognize this doxorubicin as substrate and is inhibited in the catalytic mechanism. Taken together, these two mechanisms could explain the behavior of Lipodox as a negative modulator of Pgp. We are presently analyzing if anionic liposomes loaded with other anticancer drugs

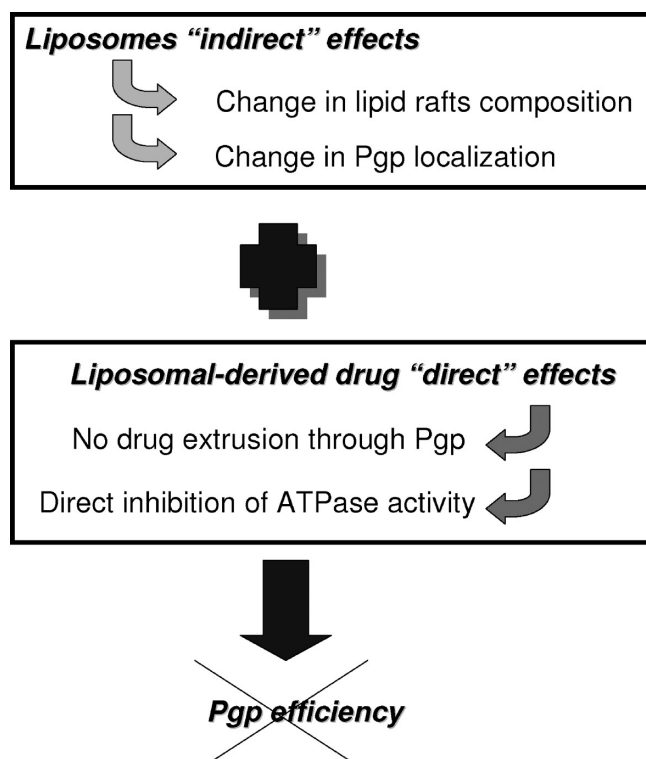


**Figure 10.** Schematic hypothetical representation of the effects of Lipodox on Pgp. The sum of indirect effects (due to the impact of liposomal shell on the membrane microenvironment) and direct effects (due to the specific interaction of the liposome-derived doxorubicin with Pgp) results in a strong and efficient inhibition of Pgp activity.

share with Lipodox the property of inhibiting Pgp and which chemical species derived from Lipodox is responsible of the direct inhibition of the pump. The knowledge of the exact mechanisms by which liposomes reverse multidrug-resistance will help to rationally design the liposomal drugs, in order to obtain precise chemophysical properties that maximally impair Pgp activity.

A first potentially translational result of our study is that, since the efficacy of Lipodox is directly linked to the expression levels of Pgp, no particular advantages in terms of anticancer efficacy, except the lesser degree of cardiotoxicity,<sup>15</sup> arise from using this doxorubicin formulation in drug-sensitive tumors. A second result derived from our study is the demonstration that genetic polymorphisms can critically affect the efficacy of Lipodox. Recently it has been reported that the C3435T single nucleotide polymorphism on *mdr1* gene improves the response rate to bortezomib plus pegylated liposomal doxorubicin in patients with multiple myeloma.<sup>48</sup> Our results show that the substitution G185 V abolishes the efficacy of Lipodox in human colon cancer cells. Therefore we suggest that routine large-scale analysis of Pgp expression and genotype could be useful, in order to design more personalized protocols based on liposomal anticancer drugs and to select *a priori* the patients who will have the major benefit from this approach.

## ■ ASSOCIATED CONTENT

**Supporting Information.** Figures S1, S2, S3, S4 and S5. This material is available free of charge via the Internet at <http://pubs.acs.org>.

## ■ AUTHOR INFORMATION

### Corresponding Author

\*Department of Genetics, Biology and Biochemistry, University of Torino, via Santena 5/bis, 10126 Torino, Italy. Phone: +390116705851. Fax: +390116705845. E-mail: chiara.riganti@unito.it.

## ■ ACKNOWLEDGMENT

We are grateful to Silvano Panero (Department of Vegetal Biology, University of Torino) for the help with the TEM analysis. We thank Paolo Olivero (Department of Experimental Physics, University of Torino, and National Institute of Nuclear Physics) for the valuable advice concerning the SEM facility, that is supported by Compagnia di San Paolo, Torino, Italy. We are indebted to Marco Minella and Claudio Minero (Department of Analytical Chemistry, University of Torino) for having provided the dynamic light scattering facility and for the valuable assistance in the interpretation of the data.

This work has been supported with grants from Compagnia di San Paolo (Programma Neuroscienze, 2008/09, Grant 2008.1136) and Ministero dell'Università e della Ricerca (MIUR, Italy).

## ■ ABBREVIATIONS USED

ABC, ATP-binding cassette; Pgp, P-glycoprotein; Lipodox, liposome-encapsulated doxorubicin; FBS, fetal bovine serum; TEM, transmission electron microscope; SEM, scanning electron microscopy; DAPI, 4',6-diamidino-2-phenylindole dihydrochloride; LDH, lactate dehydrogenase; FITC, fluorescein isothiocyanate; siRNA, small interfering RNA; GAPDH, glyceraldehyde 3-phosphate dehydrogenase

## ■ REFERENCES

- (1) Thomas, H.; Coley, H. M. Overcoming Multidrug Resistance in Cancer: An Update on the Clinical Strategy of Inhibiting P-Glycoprotein. *Cancer Control* **2003**, *10*, 159–165.
- (2) Sarkadi, B.; Homolya, L.; Szakacs, G.; Varadi, A. Human Multidrug Resistance ABCB and ABCG Transporters: Participation in a Chemoinnate Defense System. *Physiol. Rev.* **2006**, *86*, 1179–1236.
- (3) Borowski, E.; Bontemps-Gracz, M. M.; Piwkowska, A. Strategies for overcoming ABC-transporters-mediated multidrug resistance (MDR) of tumour cells. *Acta Biochim. Pol.* **2005**, *52*, 609–627.
- (4) Muñoz-Martínez, F.; Reyes, C. P.; Pérez-Lomas, A. L.; Jiménez, I. A.; Gamarro, F.; Castanys, S. Insights into the molecular mechanism of action of Celastraceae sesquiterpenes as specific, non-transported inhibitors of human P-glycoprotein. *Biochim. Biophys. Acta* **2006**, *1758*, 98–110.
- (5) Fong, W. F.; Wan, C. K.; Zhu, G. Y.; Chattopadhyay, A.; Dey, S.; Zhao, Z.; Shen, X. L. Schisandrol A from *Schisandra chinensis* reverses P-glycoprotein-mediated multidrug resistance by affecting Pgp-substrate complexes. *Planta Med.* **2007**, *73*, 212–220.
- (6) MacDiarmid, J. A.; Amaro-Mugridge, N. B.; Madrid-Weiss, J.; Sedliarou, I.; Wetzel, S.; Kocher, K.; Brahmabhatt, V. N.; Phillips, L.; Pattison, S. T.; Petti, C.; Stillman, B.; Graham, R. M.; Brahmabhatt, H. Sequential treatment of drug-resistant tumours with targeted minicells containing siRNA or a cytotoxic drug. *Nat. Biotechnol.* **2009**, *27*, 643–654.
- (7) Martin, C.; Berridge, G.; Higgins, C. F.; Mistry, P.; Charlton, P.; Callaghan, R. Communication between Multiple Drug Binding Sites on P-glycoprotein. *Mol. Pharmacol.* **2000**, *58*, 624–632.
- (8) Markman, M. Pegylated liposomal doxorubicin in the treatment of cancers of the breast and ovary. *Expert Opin. Pharmacother.* **2006**, *7*, 1469–1474.

- (9) Glas, M.; Koch, H.; Hirschmann, B.; Jauch, T.; Steinbrecher, A.; Herrlinger, U.; Bogdahn, U.; Hau, P. Pegylated liposomal doxorubicin in recurrent malignant glioma: analysis of a case series. *Oncology* **2007**, *72*, 302–307.
- (10) Jabr-Milane, L. S.; van Vlerken, L. E.; Yadav, S.; Amiji, M. M. Multi-functional nanocarriers to overcome tumour drug resistance. *Cancer Treat. Rev.* **2008**, *34*, 592–602.
- (11) Rajendran, L.; Knölker, H. J.; Simons, K. Subcellular targeting strategies for drug design and delivery. *Nat. Rev. Drug Discovery* **2010**, *9*, 29–42.
- (12) Kobayashi, T.; Ishida, T.; Okada, Y.; Ise, S.; Harashima, H.; Kiwada, H. Effect of transferrin receptor-targeted liposomal doxorubicin in P-glycoprotein-mediated drug resistant tumour cells. *Int. J. Pharm.* **2007**, *329*, 94–102.
- (13) Zalipsky, S.; Saad, M.; Kiwan, R.; Ber, E.; Yui, N.; Minko, T. Antitumour activity of new liposomal prodrug of mitomycin C in multidrug resistant solid tumour: Insights of the mechanism of action. *J. Drug Targeting* **2007**, *15*, 518–530.
- (14) Ogawara, K.; Un, K.; Tanaka, K.; Higaki, K.; Kimura, T. In vivo anti-tumour effect of PEG liposomal doxorubicin (DOX) in DOX-resistant tumour-bearing mice: Involvement of cytotoxic effect on vascular endothelial cells. *J. Controlled Release* **2009**, *133*, 4–10.
- (15) Leonard, R. C. F.; Williams, S.; Tulpule, A.; Levine, A. M.; Oliveros, S. Improving the therapeutic index of anthracycline chemotherapy: Focus on liposomal doxorubicin (Myocet<sup>TM</sup>). *Breast* **2009**, *18*, 218–224.
- (16) Visani, G.; Isidori, A. Nonpegylated liposomal doxorubicin in the treatment of B-cell non-Hodgkin's lymphoma: where we stand. *Expert Rev. Anticancer Ther.* **2009**, *9*, 357–363.
- (17) Thierry, A. R.; Vigé, D.; Coughlin, S. S.; Belli, J. A.; Dritschilo, A.; Rahman, A. Modulation of doxorubicin resistance in multidrug-resistant cells by liposomes. *FASEB J.* **1993**, *7*, 572–579.
- (18) Rahman, A.; Husain, S. R.; Siddiqi, J.; Verma, M.; Agresti, M.; Center, M.; Safa, A. R.; Glazer, R. I. Liposome-mediated modulation of multidrug resistance in human HL-60 leukemia cells. *J. Natl. Cancer Inst.* **1992**, *84*, 1909–1915.
- (19) Thierry, A. R.; Dritschilo, A.; Rahman, A. Effect of liposome on P-glycoprotein function in multidrug-resistant cells. *Biochem. Biophys. Res. Commun.* **1992**, *187*, 1098–1105.
- (20) Riganti, C.; Miraglia, E.; Viarisio, D.; Costamagna, C.; Pescarmona, G.; Ghigo, D.; Bosia, A. Nitric Oxide reverts the resistance to doxorubicin in human colon cancer cells by inhibiting the drug efflux. *Cancer Res.* **2005**, *65*, 516–525.
- (21) Riganti, C.; Doublier, S.; Aldieri, E.; Orecchia, S.; Betta, P. G.; Gazzano, E.; Ghigo, D.; Bosia, A. Asbestos induces doxorubicin resistance in MM98 mesothelioma cells via HIF-1 $\alpha$ . *Eur. Respir. J.* **2008**, *32*, 443–451.
- (22) Wong, H. L.; Bendayan, R.; Rauth, A. M.; Wu, X. Y. Development of solid lipid nanoparticles containing ionically complexed chemotherapeutic drugs and chemosensitizers. *J. Pharm. Sci.* **2004**, *93*, 1993–2008.
- (23) Provencher, S. W. A constrained regularization method for inverting data represented by linear algebraic or integral equations. *Comput. Phys. Commun.* **1982**, *27*, 213–227.
- (24) Doublier, S.; Riganti, C.; Voena, C.; Costamagna, C.; Aldieri, E.; Pescarmona, G.; Ghigo, D.; Bosia, A. RhoA silencing reverts the resistance to doxorubicin in human colon cancer cells. *Mol. Cancer Res.* **2008**, *6*, 1607–1620.
- (25) Litman, T.; Zeuthen, T.; Svovgaard, T.; Stein, W. D. Competitive, non-competitive and cooperative interactions between substrates of P-glycoprotein as measured by its ATPase activity. *Biochim. Biophys. Acta* **1997**, *1361*, 169–176.
- (26) Troost, J.; Lindenmaier, H.; Haefeli, W. E.; Weiss, J. Modulation of Cellular Cholesterol Alters P-Glycoprotein Activity in Multidrug-Resistant Cells. *Mol. Pharmacol.* **2004**, *66*, 1332–1329.
- (27) Omote, H.; Figler, R. A.; Polar, M. K.; Al-Shawi, M. K. Improved Energy Coupling of Human P-glycoprotein by the Glycine 185 to Valine Mutation. *Biochemistry* **2004**, *43*, 3917–3928.
- (28) Mizutani, T.; Hattori, A. New horizon of MDR1 (P-glycoprotein) study. *Drug Metab. Rev.* **2005**, *37*, 489–510.
- (29) Choi, K.; Chen, C.; Krieger, M.; Roninson, I. B. An altered pattern of cross-resistance in multidrug resistant human cells results from spontaneous mutation in the *mdr1* (P-glycoprotein) gene. *Cell* **1988**, *53*, 519–529.
- (30) Rao, U. S. Mutation of glycine 185 to valine alters the ATPase function of the human P-glycoprotein expressed in Sf9 cells. *J. Biol. Chem.* **1995**, *270*, 6686–6690.
- (31) Schmid, B.; Chung, D.; Warnecke, A.; Fichtner, I.; Kratz, F. Albumin-Binding Prodrugs of Camptothecin and Doxorubicin with an Ala-Leu-Ala-Leu-Linker That Are Cleaved by Cathepsin B: Synthesis and Antitumour Efficacy. *Bioconjugate Chem.* **2007**, *18*, 702–716.
- (32) Anhorn, M. G.; Wagner, S.; Kreuter, J.; Langer, K.; von Briesen, H. Specific Targeting of HER2 Overexpressing Breast Cancer Cells with Doxorubicin-Loaded Trastuzumab-Modified Human Serum Albumin Nanoparticles. *Bioconjugate Chem.* **2008**, *19*, 2321–2331.
- (33) Dalmarks, M.; Storms, H. H. A Fickian Diffusion Transport Process with Features of Transport Catalysis. Doxorubicin Transport in Human Red Blood Cells. *J. Gen. Physiol.* **1981**, *78*, 349–364.
- (34) Niu, G.; Castro, C. H.; Nguyen, N.; Sullivan, S. M.; Hughes, J. A. In vitro cytotoxic activity of cationic paclitaxel Nanoparticles on MDR-3T3 cells. *J. Drug Targeting* **2010**, *18*, 468–476.
- (35) Mamot, C.; Drummond, D. C.; Hong, K.; Kirpotin, D. B.; Park, J. W. Liposome-based approaches to overcome anticancer drug resistance. *Drug Resist. Updates* **2003**, *6*, 271–279.
- (36) Kang, D. I.; Kang, H. K.; Gwak, H. S.; Han, H. K.; Lim, S. J. Liposome composition is important for retention of liposomal rhodamine in P-glycoprotein-overexpressing cancer cells. *Drug Delivery* **2009**, *16*, 261–267.
- (37) Rosenberg, M. F.; Kamis, A. B.; Callaghan, R.; Higgins, C. F.; Ford, R. C. Three-dimensional Structures of the Mammalian Multidrug Resistance P-glycoprotein Demonstrate Major Conformational Changes in the Transmembrane Domains upon Nucleotide Binding. *J. Biol. Chem.* **2003**, *278*, 8294–8299.
- (38) Litman, T.; Zeuthen, T.; Skovsgaard, T.; Stein, W. D. Structure-activity relationships of P-glycoprotein interacting drugs: kinetic characterization of their effects on ATPase activity. *Biochim. Biophys. Acta* **1997**, *1361*, 159–168.
- (39) Orlowski, S.; Martin, S.; Escargueil, A. P-glycoprotein and 'lipid rafts': some ambiguous mutual relationships (floating on them, building them or meeting them by chance?). *Cell. Mol. Life Sci.* **2006**, *63*, 1038–1059.
- (40) Meyer dos Santos, S.; Weber, C. C.; Franke, C.; Muller, W. E.; Eckert, G. P. Cholesterol: Coupling between membrane microenvironment and ABC transporter activity. *Biochem. Biophys. Res. Commun.* **2007**, *354*, 216–221.
- (41) Klappe, K.; Hummel, I.; Hoekstra, D.; Kok, J. W. Lipid dependence of ABC transporter localization and function. *Chem. Phys. Lipids* **2009**, *161*, 57–64.
- (42) Barta, C. A.; Sachs-Barrable, K.; Feng, F.; Wasan, K. M. Effects of Monoglycerides on P-Glycoprotein: Modulation of the Activity and Expression in Caco-2 Cell Monolayers. *Mol. Pharmaceutics* **2008**, *5*, 863–875.
- (43) Liu, L.; Leonessa, F.; Clarke, R.; Wainer, I. W. Competitive and Allosteric Interactions in Ligand Binding to P-glycoprotein as Observed on an Immobilized P-glycoprotein Liquid Chromatographic Stationary Phase. *Mol. Pharmacol.* **2001**, *59*, 62–68.
- (44) Nagy, H.; Goda, K.; Fenyvesi, F.; Bacso, Z.; Szilasi, M.; Kappelmayer, J.; Lustyik, G.; Cianfriglia, M.; Szabo, G. Distinct groups of multidrug resistance modulating agents are distinguished by competition of P-glycoprotein-specific antibodies. *Biochem. Biophys. Res. Commun.* **2004**, *315*, 942–949.
- (45) Friche, E.; Demant, E. J. F.; Sehested, M.; Nissen, N. I. Effect of anthracycline analogs on photolabelling of p-glycoprotein by [<sup>125</sup>I]iodomycin and [<sup>3</sup>H]azidopine: Relation to lipophilicity and inhibition of daunorubicin transport in multidrug resistant cells. *Br. J. Cancer* **1993**, *67*, 226–231.



(46) Safa, A. R.; Sterns, R. K.; Choi, K.; Agresti, M.; Tamai, I.; Mehta, N. D.; Roninson, I. B. Molecular basis of preferential resistance to colchicine in multidrug-resistant human cells conferred by Gly-185 Val-185 substitution in P-glycoprotein. *Proc. Natl. Acad. Sci. U.S.A.* **1990**, *87*, 7225–7229.

(47) Ruth, A.; Stein, W. D.; Rose, E.; Roninson, I. B. Coordinate Changes in Drug Resistance and Drug-Induced Conformational Transitions in Altered-Function Mutants of the Multidrug Transporter P-Glycoprotein. *Biochemistry* **2001**, *40*, 4332–4339.

(48) Buda, G.; Ricci, D.; Huang, C. C.; Favis, R.; Cohen, N.; Zhuang, S. H.; Harousseau, J. L.; Sonneveld, P.; Bladé, J.; Orłowski, R. Z. Polymorphisms in the multiple drug resistance protein 1 and in P-glycoprotein 1 are associated with time to event outcomes in patients with advanced multiple myeloma treated with bortezomib and pegylated liposomal doxorubicin. *Ann. Hematol.* **2010**, *89*, 1133–1140.